FDM and Simplified FDM Solutions for MHD Viscous Nanofluid towards Stretching Sheets

Aisha Salahuddin
Regn.#203300

A thesis submitted in partial fulfillment of the requirements
for the degree of **Master of Science**

in

Mathematics

Supervised by:
Dr.Muhammad Asif Farooq

Department of Mathematics

School of Natural Sciences
National University of Sciences and Technology
H-12, Islamabad, Pakistan

2017

National University of Sciences & Technology

MS THESIS WORK

We hereby recommend that the dissertation prepared under our supervision by: AISHA SALAH UD DIN, Regn No. 00000203300 Titled: FDM & Simplified FDM Solutions For MHD Viscous Nanofluid Towards Stretching Sheets accepted in partial fulfillment of the requirements for the award of **MS** degree.

Examination Committee Members

1. Name: DR. MUJEEB UR REHMAN   Signature:

2. Name: DR. UMER SAEED   Signature:

External Examiner: PROF. MASOOD KHAN   Signature:

Supervisor's Name DR. M. ASIF FAROOQ   Signature:

_____   15-7-19
Head of Department   Date

COUNTERSINGED

Date: 15/7/2019   **Dean/Principal**

THESIS ACCEPTANCE CERTIFICATE

Certified that final copy of MS thesis written by **Ms. Aisha Salah Ud Din** (Registration No. **00000203300**), of **School of Natural Sciences** has been vetted by undersigned, found complete in all respects as per NUST statutes/regulations, is free of plagiarism, errors, and mistakes and is accepted as partial fulfillment for award of MS/M.Phil degree. It is further certified that necessary amendments as pointed out by GEC members and external examiner of the scholar have also been incorporated in the said thesis.

Signature: _____

Name of Supervisor: Dr. M. Asif Farooq

Date: 15/7/19

Signature (HoD): _____

Date: 15-7-19

Signature (Dean/Principal): _____

Date: 15/7/2019

Dedication

To my parents and respected teachers.

Acknowledgements

Completion of this thesis was not entirely an effort of a single person rather it is the effort of number of individuals. I would like to acknowledge some significant people for their support in the completion of this thesis.

All of me and my efforts are for Allah to whom I am thankful. The foremost among all individuals is my supervisor Dr.Muhammad Asif Farooq who guided me on every step and helped me overcome every hurdle that stood before me. I owe him alot for converting my mere dream into reality. I would not have been able to do this task if it had not been for Sir Asif who took time out of his busy schedule.

I would like to thank my family for their sincere concern and devoted prayers throughout my research phase. A special thanks to my parents who was always there to encourage me at times of need.

Finally I would like to thank whole faculty and staff of my department for providing best possible environment to the students.

Abstract

The investigation presented in this thesis is a theoretical study of radiating MHD nanofluid past a slippery stretchable surfaces immersed in a porous medium. The main motivation behind this study is bi-folds. Firstly, to seek the behavior of nanofluids under the effect of MHD, buoyancy, porosity, Joule heating, thermal radiation, secondly, to present a new strategy applicable on the resultant PDEs for finding its numerical solution. In first problem, the resulting equations are in the form of nonlinear partial differential equations, we will convert PDES by means of similarity variables to obtain an alternative set of PDES with less number of dependent variables. To obtain numerical solution we lower the order of the resultant PDEs by introducing a new variable for the first order partial derivative then use the finite difference approximation on the resultant lower order PDEs. For spatial discretization we apply first order method. For time integration we use the first order explicit Euler method. In second problem, the governing equations of motion under considerations are framed as partial differential equations (PDEs) and afterward changed into an ordinary differential equations (ODEs) through consolidating similarity transformations. We attempt to develop a novel numerical procedure, the simplified FDM which uses LU-Factorization. The effectiveness of this scheme is verified by comparing its solution with literature and in case the solution does not exist we compare it with the computational outcome gained from MATLAB built-in package *bvp4c*. The pose processing of relevant data for velocity, temperature and, concentration has been tabulated and graphed for a variety of parameters i.e. Prandtl, Grashof and thermal radiation parameters, Darcy, Eckert and Lewis numbers, thermophoresis and Brownian parameters. The significant impact of the associated emerging thermophysical parameters i.e. roughness of wall (skin friction coefficient) and local heat flux (local Nusselt number) and local concentration flux (local Sherwood number) at the wall have been examined.

Contents

List of Abbreviations

$(u,\ v)$ the velocity components

μ the coefficient of viscosity

ρ the density of fluid

σ the electrical conductivity of the fluid

T fluid temperature

T_0 reference temperature

K the porous medium permeability

β the thermal expansion coefficient

k the thermal conductivity

C_p the specific heat capacity

q_r the radiative heat flux

Q the heat source coefficient

C the concentration

τ time

$(\rho C)_p$ heat capacities of nanofluid

$(\rho C)_f$ heat capacities of base fluid

C_p the specific heat at constant pressure

D_B Brownian coefficients

D_T thermophoretic diffusion coefficients

T_∞ the ambient fluid temperature

C_∞ the ambient fluid concentration

Pr   Prandtl number

Gr   Grashof number

Le   Lewis number

Nt   thermophoresis number

Nb   Brownian motion parameter

λ Slip parameter

S   Heat source parameter

Nr   thermal radiation parameter

Ec   Eckert number

Da   Darcy number

M   Magnetic parameter

List of Figures

List of Tables

Chapter 1

Introduction

Fluid mechanics concerned with the effects resulted from forces and energy due to fluid flow. The subject of fluid mechanics can be partitioned into two branches: statics and dynamics. There are numerous applications particularly dedicated to development of fluid dynamics. This may include some of interesting fields of engineering such as mechanical engineering (hydraulic press, hydralic brakes etc), electrical engineering (semi conductor industries) and chemical (centrifuges) etc.

1.1 Literature Review

The fluid flow due extended sheet has been deliberated due to its different engineering applications such as in chemical engineering for the polymer processing unit, and in metallurgy. Crane [1] examined 2-D boundary-layer stream due to extending (stretching) the sheet in a steady state, which moves in its own plane with a velocity that changes directly with the distance from a fixed point on it. Immediately after Crane [1] abundant work in this direction reported and discussed.

The result of boundary layer stream over linearly extending (stretching) sheet of nanofluid was explored by Makinde and Aziz [2] whilst Mustafa et al. [3] focused on boundary layer flow over an exponentially extending sheet and utilized homotopy analysis method for the computation of analytical solutions. Practically, extending of

a plastic sheet may not essentially be linear as discussed by Gupta and Gupta [4].

As off late the nanofluid suspension take critical consideration after a study by Choi and Eastman [5] as heat exchange rate of common liquids have low thermal conductivity and this causes the system to operate inefficiently as well as consume extra energy to provide useful results. A new method has been introduced to optimize machine operation by dispersing solid particles with a base fluid. Nanofluid is a mixing of conventional base fluids like water, motor oil, etc with nanometer sized solid particles. A comprehensive review of the literature about nanofluid is given by references from [2], [3], [5]. Sheikholeslami and Bhatti [6] investigated the impact of nanoparticles considering distinctive shapes in convection flows. Recently Sheikholeslami [7] considered the Brownian movement and its impact on nanofluid flow interior of a permeable cavity.

The study of flow of an electrically conducting fluid has many applications in engineering problems such as in MHD generators, plasma studies, nuclear reactors, geothermal energy extraction, and the boundary layer control in the field of aerodynamics [8]. Consequences of frictional and irregular heat on MHD non-Newtonian fluid flows due to stretched surface was studied by Reddy et al. [9].

Dual solutions of mixed convection flow with momentum and thermal slip over a permeable shrinking cylinder has been discussed by Mishra and Singh [10]. When a study is carried out in smaller scales (i.e. 10^{-9}) the process is mostly influenced by slip flow. This observation has been varified in Hadjiconstantinou [11] [12] where some slip parameter have been introduced. The slip coefficients are thus outcome of the aforementioned analysis. Researchers usually favours slip flow phenomena. Fang et al. [13] proposed second order slip flow model in their study above a porous shrinking sheet. Ullah et al. [14] examined two-dimensional Reiner-Philippoff fluid model in the presence of radiation while considering unsteady surface.

Thermal radiation and viscous dissipation effects on the unsteady boundary layer flow of nanofluid over a stretching sheet were presented by Khan et al. [15]. In this study they accounted for viscous dissipation effect and found that raising the values of Eckert number enlarges the thermal boundary layer thickness. Ibrahim and Shankar [16] analyzed the influence of thermophoresis on Brownian motion of a MHD fluid due to a stretching sheet.

There are several technological devices that relay on buoyancy effect. Makinde et al [17] studied combined effects of buoyancy force, convective heating, Brownian motion, thermophoresis and magnetic field on stagnation point flow and heat transfer due to nanofluid flow towards a stretching sheet. Ali and Yousef [18] investigated laminar mixed convection flow in vertical surface. Partha et al. [19] studied mixed convection heat transfer from an exponentially stretching sheet. Viscous dissipation in naturally convective system is investigated in Gebhart [20], Gebhart and Mollendorf [21]. Combination of analytical and numerical for exponentially vertical surface has been investigated in Magyari and Keller [22]. Unsteady flow of thermally radiating nanofluid over non-linearly surface was discussed in Seth et al. [23]. They observed the velocity curve of the nanofluid is dependent on the unsteadiness, velocity slip and the nonlinearity of the stretching velocity. Makinde et al. [24] make a systematic analysis by using FDM technique for MHD fluid over a slippery surface through a porous medium. Hashim et al. [25] have discussed the thermophysical properties of the flow of Williamson nanofluid and solved their problem numerically. They concluded that the stronger the magnetic field resulted in decreasing of boundary layer thickness. Some other references in this direction can be consulted in [26], [27], [28].

The entropy generation of nanofluid due to a magnetic field over a stretching surface earnestly efforted by Qing et al. [29]. Hosseini et al. [30] discussed heat transfer of nanofluid flow in micro channel heat sink (MCHS) in the presence of a magnetic field. The influence of chemical reaction and heat generation/absorption on mixed convective flow of nanofluid past an exponentially stretched surface has been examined

3

by Eid [31] ,and numerical solutions has been obtained by utilizing the shooting technique along with Runge-Kutta-Fehlberg method. Afify and Elgazery [32] investigated numerically, the boundary layer flow of Maxwell nanofluid with convective boundary condition and heat absorption. Reviews of viscous fluid flow problems for non-linear stretching sheet have been presented Prasad et al. [33], Afzal [34], and Nandeppanavar et al. [35]. Nadeem and Lee [36] studied analytically the problem of steady boundary layer flow of nanofluid over an exponentially stretching surface including the effects of Brownian motion and thermophoresis parameters. The application of solar energy with Hiemenz flow of nanofluid over a wedge discussed by Mohamad et al. [37]

In all previous studies a usual course is followed in one way or the other and discussion is intended towards linearly or nonlinearly stretching sheets in the absence of some important emerging parameters. We perform current study to fill this gap by introducing relevant physical forces and discussing a very important fluid commonly called nanofluid. Another aim of this work is to add new numerical methodology in the literature so that it can applicable to many problems. For that here we develop the simplified FDM which gives good results. To the best of our knowledge the current mathematical model is not considered before and added to that the simplified FDM has not been applied in the literature. It was found that some of the parameters have an important effect on the boundary layer thickness. The governing equations with suitable boundary conditions are mathematically transformed into a non-linear partial differential equations by exercising similarity variables and then tackle the resulting problem by suitable numerical schemes.

1.2   Basic Definitions and Preliminaries

This section begin with some basic concepts and definitions.

1.2.1   Fluid Mechanics

Fluid cannot resist shearing forces and deform continuously under applied stress no mater how small it is.

Fluid mechanics is particularly the study of behavior of the fluid flows followed by stationary mode (fluid static) or in dynamic mode (fluid dynamic). It is a branch of classical physics with applications of great importance in hydraulic and aeronautical engineering, chemical engineering, meteorology, and zoology. Scientists across several fields study fluid dynamics. Fluid dynamics provides methods for studying the evolution of stars, ocean currents, weather patterns, plate tectonics and even blood circulation. Some important technological applications of fluid dynamics include rocket engines, wind turbines, oil pipelines and air conditioning systems

1.2.2   Incompressible

Term incompressible refer to not being reduced by force or applied pressure is incapable of reduction of density.

1.2.3   bvp4c

To determine the solution of fairly sophisticated boundary value problem directly we use routine, known as bvp4c. An initial estimate is required in Matlab programming bvp4c algorithm. It is based on collocation and solution starts with initial estimate provided initial mesh points. and the collocation polynomial provides a C1-continuous solution that is fourth order accurate uniformly in [a,b]. Residual of the continuous solution provide Mesh selection and error control.

1.2.4   FDM

Boundary value problem will be treated with the help of Finite Difference method. This is accomplished by replacing each derivative in Differential equation using appropriate difference quotient approximation with step size h. Specified order of truncation error

is maintained by step size h. Thus differential equation is reduced to system of algebraic equations which is then solved on digital computer.

To introduce the concept, consider $f(x)$ as a continuous function on $[a \ b]$. For a positive integer N, we divide domain $[l_1 \ l_2]$ into equal subintervals with whose meshpoints $z_i = l_1 + ih$, for $i = 0, 1, ..., N + 1$, where $\Delta z = \frac{(l_1 - l_2)}{(N+1)}$. For three arbitrary points, z_{i+1}, z_i and z_{i-1} with corresponding ψ_{i+1}, ψ_i and ψ_{i-1}. Expanding ψ about z_i on $[z_{i+1} \ z_{i-1}]$ by Taylor polynomial we have

$$\psi(z_{i+1}) = \psi(z_i + h) = \psi(z_i) + h\psi'(z_i) + \frac{h^2\psi''(z_i)}{2!} + \frac{h^3\psi'''(C_1)}{3!}, \tag{1.1}$$

for some $C_1 \in (z_{i-1} \ zi + 1)$,

$$\psi(z_{i-1}) = \psi(z_i - h) = \psi(z_i) + h\psi'(z_i) - \frac{h^2\psi''(z_i)}{2!} + \frac{h^3\psi'''(C_2)}{3!}, \tag{1.2}$$

for some $C_2 \in (x_{i-1} \ x_{i+1})$, solving for ψ'' add Eqn (1.1) and (1.2) we have,

$$\psi''(z_i) = \frac{1}{h^2}[\psi(z_{i+1}) - \psi(z_{i-1})] - \frac{h^2}{24}[\psi'''(C_1) - \psi'''(C_2)], \tag{1.3}$$

error term is simplified by using intermediate value theorem,

$$\psi''(z_i) = \frac{1}{h^2}[\psi(z_{i+1}) - \psi(z_{i-1})] - \frac{h^2}{24}[\psi'''(C))], \tag{1.4}$$

for some $C \in (z_{i-1} \ z_{i+1})$, to get first order finite difference derivative we have,

$$\psi(z_{i+1}) = \psi(z_i + h) = \psi(z_i) + h\psi'(z_i) + \frac{h^2\psi''(C_1)}{2!}, \tag{1.5}$$

solving for f', using forward difference, we get,

$$\psi'(z_i) = \frac{\psi(z_{i+1}) - \psi(z_i)}{h} - \frac{h}{2}\psi(C_1), \tag{1.6}$$

$$\psi(z_{i+1}) = \psi(z_i + h) = \psi(z_i) + h\psi'(z_i) + \frac{h^2\psi''(C_1)}{2!}, \tag{1.7}$$

for some $C_1 \in (z_i \ z_{i+1})$,

and by using backward difference, we get,

$$\psi(z_{i-1}) = \psi(z_i - h) = \psi(z_i) - h\psi'(z_i) + \frac{h^2\psi''(C_2)}{2!}, \qquad (1.8)$$

$$\psi'(z_i) = \frac{\psi(z_i) - \psi(z_{i-1})}{h} - \frac{h}{2}\psi(C_2), \qquad (1.9)$$

for some $C_2 \in (z_{i-1} \quad z_i)$, In equation (1.4), the truncated error is of 2nd-order and in equation (1.6) and (1.9), the truncated error is of 1st-order.

1.2.5 Prandlt Number

Prandlt number or Pr is known to be a dimensionless parameter, and it is effective when we talk about the heat transfer between fluid flow and solid body. Prandlt number is therefore a ratio of molecular diffusivity of momentum to the molecular diffusivity of heat. Mathematically

$$Pr = \frac{C_p\nu}{k},$$

$$Pr = \frac{\nu}{\alpha} = \frac{\frac{\mu}{\rho}}{\frac{k}{\rho C_p}},$$

Therefore,

$$Pr = \frac{\text{Momentum difusivity}}{\text{Thermal difusivity}}.$$

Prandlt number is important in heat transfer flows. It is used in calculation of momentum and thermal boundary layer thickness. Thermal diffusivity dominates for small values of Prandtl number whereas for large values viscous diffusivity dominates.

1.2.6 Grashoff Number

A dimensionless number Grashof number or simply Gr approximates the ratio of the buoyancy to viscous force acting on a fluid. Accordingly Gr is a way, due to which we can quantify the opposing force. Thus Gr is defined as

$$Gr = \frac{g\beta(T_{wall} - T_\infty)L^3}{\nu^3}.$$

7

1.2.7 Thermeophresis

Particle motion in a temperature gradient, from a hotter to a colder region Thermophoresis is a force that arises from particle motion from a hotter to a colder region due to a temperature gradient.

$$Nt = \frac{\tau D_T (T_w - T_\infty)}{T_\infty \nu}.$$

1.2.8 Brownien Motion

Random fluctuation of particle in fluid suspension constantly undergoing collision with atoms or molecules. Any factor impact the pattern of motion may affect the rate of Brownian motion e.g increased temperature gradient, increased nanoparticle volume fraction, shape and size of particle and viscosity.

$$Nb = \frac{\tau D_B (C_w - C_\infty)}{\nu}.$$

1.2.9 Eckert Number

Eckert number is defined as

$$Ec = \frac{u^2}{\Delta T C_p}.$$

Eckert number is momentous where the viscous dissipation is prominent such as high speed flows. With Ec approximately 0.3 transfer of heat is at maximum level which is of great interest for cooling of hot surface in a flow as mentioned in [49].

1.2.10 Lewis Number

The dimensionless parameter Lewis number defined as the ratio of thermal diffusivity to mass diffusivity. It is used to characterize fluid flows where there is simultaneous heat and mass transfer.

$$Le = \frac{\nu}{D_B}.$$

8

1.2.11 Skin friction coefficient

A dimensionless number characterizing the frictional force at the boundary between fluid and a wall. The skin friction coefficient C_f is defined as

$$C_f = \frac{\tau_w}{\rho u_w^2}, \qquad \text{where} \qquad \tau_w = \mu \frac{\partial u}{\partial y}.$$

1.2.12 Local Nusselt Number

Nusselt number Nu_x is defined as:

$$Nu_x = \frac{x q_w}{k(T_w - T_\infty)}, \qquad \text{where} \qquad q_w = -k(1 + \frac{16\sigma^* T_\infty^3}{3k^* k})\frac{\partial f}{\partial y}.$$

1.2.13 Sherwood Number

The Sherwood number sh_x is defined as: the local Sherwood number Sh_x is given by

$$Sh_x = \frac{x j_w}{k(C_w - C_\infty)}, \qquad \text{where} \ \ j_w = -D \frac{\partial C}{\partial y}\big|_{y=0}.$$

1.2.14 Applications of nanofluid

An ultra fine mixture of nanometer sized particle suspended in base fluid forming homogeneous suspension is referred as nanofluid. Nanomaterials have plentiful and inclusive applications in several engineering and industrial sectors. Due to their enhanced thermal conductivity nanofluid are used as coolant in different devices such as heat exchangers, electronic cooling system, coolent for transformer and for nuclear reactor plant, for cancer treatment as radiation therapy.

Chapter 2

Boundary layer flow of hydromagnetic radiating fluid over linearly stretching sheet embedded in porous medium

This chapter discusses the review work of Makinde et al. [24]. The main focus of this chapter is to study boundary layer flow of hydromagnetic radiating fluid over a linearly stretching sheet immersed in porous medium in two dimensional unsteady processes. The study analyze all parameters such as Prandtl number, Grashof number, thermal radiation, magnetic field, viscous dissipation, heat source or sink and Darcy number has been employed. Here the compatible numeric scheme is employed to solve the system of non-linear partial differential equations which exemplify the effects of hydromagnetic radiating fluid flow over slippery stretching surface. The study reveals that solution converge well for different parameters pertaining significant effects on flow field regime.

The chapter has been arranged as follows. In Section 2.1, mathematical formulation is presented. In Section 2.2, the solution strategy have been discussed. At the end results are shown in graphical form.

2.1   Governing Equations

Here we give heat transfer features of hydromagnetic radiating fluid past a slippery stretching surface immersed porous medium. A constant strength magnetic field, B_0

is imposed perpendicular to the sheet. While studying the flow phenomenon we make following assumptions.

1. Heat source

2. Buoyancy force

3. Thermal radiation

4. Darcy's Law

The governing equations are expressed as [38]:

Conservation of Mass:

$$\partial_x u + \partial_y v = 0, \tag{2.1}$$

Conservation of Momentum:

$$u_t + u u_x + v u_y = \nu u_{yy} - \frac{\sigma B_0^2 u}{\rho} - \frac{\nu u}{K} + g\beta(T - T_\infty), \tag{2.2}$$

Conservation of Energy:

$$T_t + u T_x + v T_y = \frac{k}{\rho C_p} T_{yy} + \frac{\nu}{C_p}(u_y)^2 + \frac{\sigma B_0^2 u^2}{\rho C_p} + \frac{\nu u^2}{C_p K} - \frac{1}{\rho C_p} q_{r,y} + \frac{Q(T - T_\infty)}{\rho C_p}. \tag{2.3}$$

The related initial and boundary conditions are written as:

$$(u, v, T) = (0, 0, T_\infty) \qquad \text{at} \quad t = 0, \tag{2.4}$$

$$(u, v, T) = (u_w + \frac{\mu}{L} u_y, 0, T_w) \quad \text{at} \quad y = 0, \tag{2.5}$$

$$(u, T) \to (0, T_\infty) \qquad as \quad y \to \infty, \tag{2.6}$$

where u is the velocity component in x-direction and v is the velocity component in y-direction. We assume $u = u_w = ax$ as a surface velocity, the coefficient of slip

11

length is L, wall temperature is $T_w = T_\infty + bx$. Here t and T represents time and temperature respectively. We denote C_p as the specific heat, permeability is denoted by K and k is the thermal conductivity of fluid, heat source coefficient by Q. Moreover, ρ, σ, β, μ and ν stands for the density, fluid electrical conductivity, thermal expansion coefficient, fluid dynamic viscosity and fluid kinematic viscosity, respectively. The Roseland approximation for a radiative heat flux have been considered in this work [39], [40], [41], [42] and [43].

Introducing following similarity variables to transform the above equations (2.1), (2.2) and (2.3).

$$\psi = (a\nu)^{\frac{1}{2}} x f, \quad \eta = \left(\frac{a}{\nu}\right)^{\frac{1}{2}} y, \quad \theta = \frac{T - T_\infty}{T_w - T_\infty}, \tag{2.7}$$

the connection between the components of velocity with stream function is written as:

$$u = \psi_y, \quad v = -\psi_x, \tag{2.8}$$

Using Eq. (2.8) the velocity components in x- and y-direction in the form of u and v can be written as:

$$u = axf_\eta, \quad v = -(a\nu)^{\frac{1}{2}} f. \tag{2.9}$$

By using these similarity variables we establish following nonlinear third order partial differential equations:

$$\frac{\partial^2 f}{\partial \eta \partial \tau} - \frac{\partial^3 f}{\partial \eta^3} - f\frac{\partial^2 f}{\partial \eta^2} + \left(\frac{\partial f}{\partial \eta}\right)^2 + \left(M + \frac{1}{Da}\right)\frac{\partial f}{\partial \eta} - Gr\theta = 0, \tag{2.10}$$

$$Pr\frac{\partial \theta}{\partial \tau} + Pr\left(\theta\frac{\partial f}{\partial \eta} - f\frac{\partial \theta}{\partial \eta}\right) - (1 + Nr)\frac{\partial^2 \theta}{\partial \eta^2} - EcPr\left(\frac{\partial^2 f}{\partial \eta^2}\right)^2$$
$$-EcPr\left(M + \frac{1}{Da}\right)\left(\frac{\partial f}{\partial \eta}\right)^2 - PrS\theta = 0, \tag{2.11}$$

where Da, Gr, Pr, Nr, M, Ec and S are Darcy's number, Grashof number, radiation parameter, magnetic field strength, Eckert number and heat source, respectively. These

12

parameters are defined as:

$$Re_x = \frac{u_w x}{\nu}, \quad \tau = at, \quad Gr = \frac{\beta g b}{a^2}, \quad M = \frac{\sigma B^2}{\rho a}, \tag{2.12}$$

$$Da = \frac{Ka}{\nu}, \quad Ec = \frac{au_w}{bC_p}, \quad Pr = \frac{\rho \nu C_p}{k}, \quad S = \frac{Q}{a\rho C_p}, \quad \nu = \frac{\mu}{\rho}, \tag{2.13}$$

with corresponding conditions are given below:

$$(f_\eta, f, \theta) = (0, 0, 0) \quad \text{at} \quad \tau = 0, \tag{2.14}$$

$$(f_\eta, f, \theta) = (1 + \lambda f_{\eta\eta}, 0, 1) \quad \text{at} \quad \eta = 0, \tag{2.15}$$

$$(f_\eta, \theta) \to (0, 0) \quad \text{as} \quad \eta \to 0, \tag{2.16}$$

where λ is the slip parameter. The important non-dimensional quantities are given by

$$C_f = \frac{\tau_w}{\rho u_w^2}, \quad \text{where} \quad \tau_w = \mu u_x, \tag{2.17}$$

$$Nu_x = \frac{x q_w}{k(T_w - T_\infty)}, \quad \text{where} \quad q_w = -k(1 + \frac{16\sigma^* T_\infty^3}{3k^* k})T_y, \tag{2.18}$$

where C_f is skin friction coefficient, τ_w is shear stress, Nu is local nusselt number and q_w is heat flux. We have

$$\sqrt{Re_x} C_f = f_{\eta\eta}(0, \tau), \tag{2.19}$$

$$\frac{Nu_x}{\sqrt{Re_x}} = -(1 + Nr)\theta_\eta(0, \tau). \tag{2.20}$$

2.2 Numerical Scheme

Here we find numerical solution of dimensionless non-linear PDEs (2.10) and (2.11) with corresponding boundary conditions (2.14) to (2.16), an explicit finite difference method (FDM) algorithm, as described in detail in [44]. In order to approach the solution, a rectangular region is chosen for a flow field which is divided into mesh of

13

lines. While considering boundary layer assumptions, the change in flow pattern is insignificant in x-direction as compared to y-direction. The discretization of PDEs is given below.

Discretization:

It is assumed that $\Delta\eta$, $\Delta\tau$ are constant mesh size prescribed as $\Delta\eta = \frac{\eta_\infty}{N}$ $(0 < \eta < \eta_\infty)$ and $\Delta\tau = \frac{\tau_{end}}{n_{end}}$ $(0 < \tau < \tau_{end})$. The subscripts i and n designate the mesh points of coordinates (η, τ) as (η_i, τ_n) where $\eta_i = i\Delta\eta, i = 0, 1, ..., N$ and $\tau_n = n\Delta t, n = 0, 1, 2, ...$In explicit approach, the finite difference stencil is shown in Figure ??.

For discretization in η-direction, we apply backward finite difference approximation for first order derivatives and central difference approximations for second order derivative. For time integration, we use explicit Euler method. For implementation of FDM in MATLAB, we reduce the order of momentum equation and the temperature equations have not been reduced since it is already second order. All the finite difference approximation of all derivative is given below. Now we explain the procedure to reduce the order of the unsteady momentum equation. We assume $\frac{\partial f}{\partial \eta} = F$ then the Eqns (2.10)-(2.11) takes the following form:

$$\frac{\partial F}{\partial \tau} - f\frac{\partial F}{\partial \eta} - \frac{\partial^2 F}{\partial \eta^2} + (F)^2 + (M + \frac{1}{Da})F - Gr\theta = 0, \tag{2.21}$$

$$Pr\frac{\partial \theta}{\partial \tau} + Pr(\theta F - f\frac{\partial \theta}{\partial \eta}) - (1 + Nr)\frac{\partial^2 \theta}{\partial \eta^2} - EcPr(\frac{\partial F}{\partial \eta})^2$$
$$- EcPr(M + \frac{1}{Da})(F)^2 - PrS\theta = 0, \tag{2.22}$$

The order of associated boundary conditions (2.14)-(2.16) reduces as follows:

$$(F, f, \theta) = (0, 0, 0), \quad \text{at} \quad \tau = 0 \tag{2.23}$$

$$(F, f, \theta) = (1 + \lambda F_\eta, 0, 1), \quad \text{at} \quad \eta = 0 \tag{2.24}$$

$$(F, \theta) \to (0, 0), as \quad \eta \to \infty \tag{2.25}$$

14

i - 1, n + 1   i, n + 1   i + 1, n +1

i - 1, n   i, n   i + 1, n

i - 1, n - 1   i, n - 1   i + 1, n -1
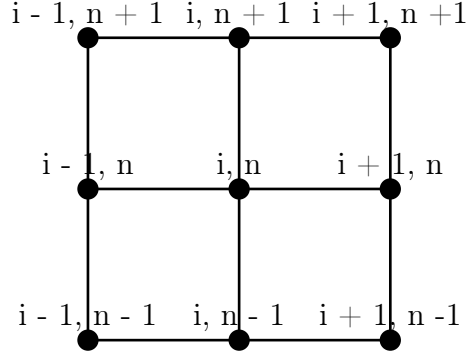
Figure 2.1: stencil for FDM.

In order to find a solution, we approximate the derivative appears in the partial differential equations (PDEs) by linear combinations of function values at the grid points by using the finite difference method (FDM). All the finite difference approximation of all orders are given by :

$$\left(\frac{\partial F}{\partial \eta}\right)_{(i,n)} = \frac{F_{i+1}^n - F_i^n}{\Delta \eta}, \quad \left(\frac{\partial^2 F}{\partial \eta^2}\right)_{(i,n)} = \frac{F_{i+1}^n - 2F_i^n + F_{i-1}^n}{(\Delta \eta)^2}, \quad \left(\frac{\partial F}{\partial \tau}\right)_{(i,n)} = \frac{F_i^{n+1} - F_i^n}{\Delta \tau},$$

$$\left(\frac{\partial \theta}{\partial \eta}\right)_{(i,n)} = \frac{\theta_{i+1}^n - \theta_i^n}{\Delta \eta}, \quad \left(\frac{\partial^2 \theta}{\partial \eta^2}\right)_{(i,n)} = \frac{\theta_{i+1}^n - 2\theta_i^n + \theta_{i-1}^n}{(\Delta \eta)^2}, \quad \left(\frac{\partial \theta}{\partial \tau}\right)_{(i,n)} = \frac{\theta_i^{n+1} - \theta_i^n}{\Delta \tau}.$$

Here superscript $'n'$ and $'n+1'$ denotes the solution at n^{th} and $(n+1)^{th}$ time levels. And i, $i-1$ and $i+1$ is the location of the solution at current, previous and forward locations. Inserting all these approximation into the above equations Eqs. (2.24) and (2.25)

$$\frac{F_i^{n+1} - F_i^n}{\Delta\tau} - \frac{F_{i+1}^n - 2F_i^n + F_{i-1}^n}{(\Delta\eta)^2} - f_i^n \frac{F_{i+1}^n - F_i^n}{\Delta\eta} + (F^n)^2$$
$$+(M + \frac{1}{Da})\frac{F_{i+1}^n - F_i^n}{\Delta\eta} - Gr\theta_i^n = 0,$$

$$Pr\frac{\theta_i^{n+1} - \theta_i^n}{\Delta\tau} + Pr\theta_i^n F_i^n - Prf_i^n(\frac{\theta_{i+1}^n - \theta_i^n}{\Delta\eta}) - (1 + Nr)\frac{\theta_{i+1}^n - 2\theta_i^n + \theta_{i-1}^n}{(\Delta\eta)^2}$$
$$-EcPr(\frac{F_{i+1}^n - F_i^n}{\Delta\eta})^2 - EcPr(M + \frac{1}{Da})(F_i^n)^2 - PrS\theta_i^n = 0,$$

The initial and boundary conditions involved reads as

$$\tau = 0: \quad F_i^0 = 0, \quad f_i^0 = 0, \quad \theta_i^0 = 0,$$

$$\eta = 0: \quad F_0^n = 1 + \lambda\frac{F_0^n - 2F_0^n + F_0^n}{(\Delta\eta)}, f_0^n = 0, \quad \theta_0^n = 1,$$

$$\eta = \infty: \quad F_{\eta\infty}^n = 0, \quad \theta_{\eta\infty}^n = 0.$$

The local Nusselt number and the skin friction coefficient for finite difference implementation read as:

Local Nusselt Number:

$$\frac{Nu_x}{\sqrt{Re_x}} = -(1 + Nr)\frac{\theta_1^n - \theta_0^n}{\Delta\eta}.$$

Skin Friction Coefficient

$$\sqrt{Re_x}C_f = \frac{F_1^n - F_0^n}{(\Delta\eta)}.$$

2.3   Results and Discussions

Throughout this work, the effects of hydromagnetic radiating fluid flow over a slippery stretching sheet have been studied both analytically and numerically. The observed

16

response against Magnetic strength and time for velocity and temperature can be observed in Figure 2.2(a) and 2.2(b). Initially, velocity remains low in the absence of Magnetic strength then increase with time ofterwords. Incremental M reduce hydrodynamic boundary layer thickness, but eventually thickness increases with time. Both magnetic field and time causes an increase in thermal boundary layer thickness. The Grashof number and Darcy's number effects on dimensionless velocity and temperature are shown in Figure 2.3(a) and 2.3(b). When $Ec = 0$ the dimensionless velocity is highest and then decrease with increasing slip parameter but the reverse effects can be seen in temperature profile which can be observe in Figure 2.4(a)and 2.4(b).
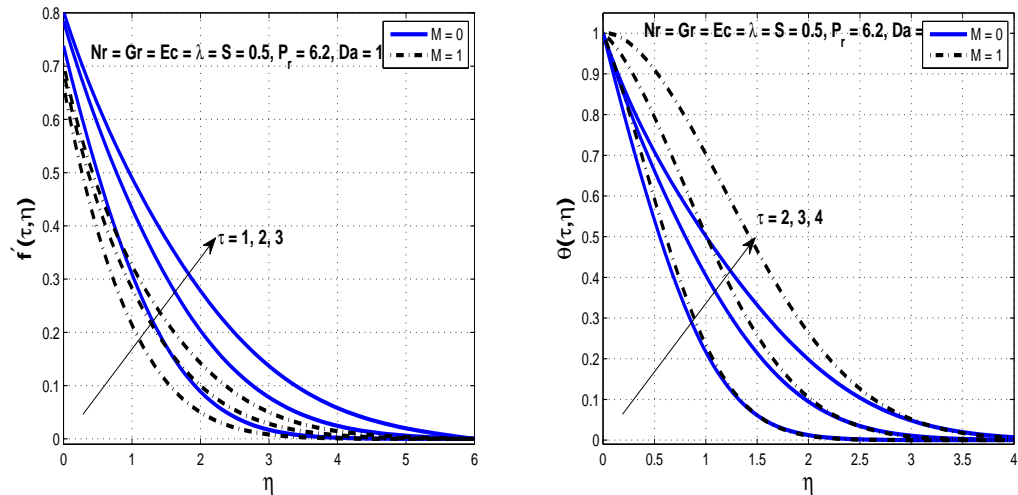
Figure 2.2: Impact of magnetic field with incremental time on velocity and temperature curve.
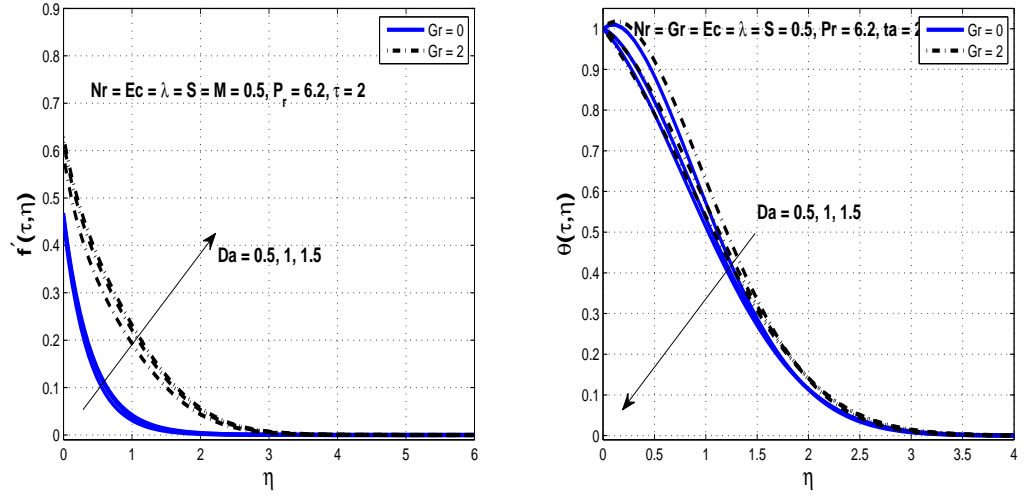
Figure 2.3: Impact of Grashof number with incremental Darcy on velocity and temperature curve.
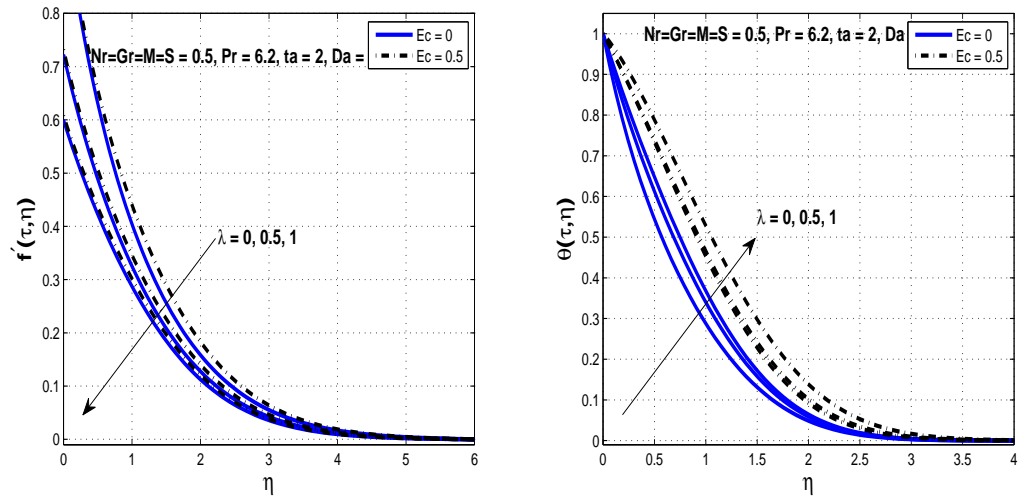
Figure 2.4: Impact of Eckert number with incremental slip parameter on velocity and temperature curve.

Chapter 3

FDM for Unsteady MHD Radiating Nanofluid Flow past a Stretchable Surface Immersed in a Permeable Medium

Here, we present the main two goal. To examine convenient effects of MHD, buoyancy, porosity, Joule heating, thermal radiation within flow field and to present a new strategy to solve PDEs.

The overall structure of the chapter is as follows. Section 3.1 begins by laying out the mathematical description of the physical problem. Methodology is presented in section 3.2. The spatial and temporal discretizations of PDEs have been given in Section 3.3. Interpretations of the results have been discussed in Section 3.4.

3.1   Mathematical Model

Here we consider the two dimensional, time dependent, laminar, incompressible, hydromagnetic radiating nanofluid induced by linearly stretching sheet submerged in a porous medium. In the light of above mentioned assumptions we extend the earlier formulation of Makinde et al [24].

19

Conservation of Mass:

$$\partial_x u + \partial_y v = 0, \tag{3.1}$$

Conservation of Momentum:

$$u_t + u u_x + v u_y = \nu u_{yy} - \frac{\sigma B_o^2 u}{\rho} - \frac{\nu u}{K} + g\beta(T - T_\infty), \tag{3.2}$$

Conservation of Energy:

$$T_t + u T_x + v T_y = \frac{k}{\rho C_p} T_{yy} + \frac{\nu}{C_p}(u_y)^2 + \frac{\sigma B_o^2 u^2}{\rho C_p} + \frac{\nu u^2}{C_p K} - \frac{1}{\rho C_p} q_{r,y}$$
$$+ \frac{Q(T - T_\infty)}{\rho C_p} + \tau[D_B(C_y T_y) + \frac{D_T}{T_\infty}(T_y)^2], \tag{3.3}$$

Conservation of Concentration:

$$C_t + u C_x + v C_y = D_B C_{yy} + \frac{D_T}{T_\infty} T_{yy}, \tag{3.4}$$

where (u, v) are the components of velocity in x and y directions. μ is the coefficient of viscosity, ρ denotes the density of the fluid, σ is the electrical conductivity of the fluid, T is fluid temperature, K is the permeability of porous medium, β is the thermal expansion coefficient, k is the thermal conductivity, C_p is the specific heat capacity, q_r is the radiative heat flux, Q is the heat source coefficient, C is the concentration, $\tau = (\rho C)_p/(\rho C)_f$ here $(\rho C)_p$, $(\rho C)_f$ are heat capacities of nanofluid and base fluid respectively, C_p is the specific heat at constant pressure, D_B, D_T are Brownian, thermophoretic diffusion coefficients, respectively. T_∞ is the ambient fluid temperature and C_∞ is the ambient fluid concentration.

3.1.1 Boundary Conditions

The preceding mathematical model allow the following boundary condition:

$$(u, v, T, C) = (0, 0, T_\infty, C_\infty) \quad \text{at} \quad t = 0,$$
$$(u, v, T, C) = (U_w + \frac{\mu}{L} u_y, 0, T_w, C_w), \quad \text{at} \quad y = 0,$$
$$(u, T, C) = (0, T_\infty, C_\infty) \quad \text{as} \quad y \to 0, \tag{3.5}$$

Here we consider $u_w = ax$ as a stretching velocity, $T_w = T_\infty + bx$ is the variable temperature at sheet with T_∞ being a free stream constant and $C_w = C_\infty + cx$ is the variable concentration of nanofluid at the sheet with C_∞ being a constant.

3.2 Method of Solution

Introducing following similarity variables to transform the momentum, energy and concentration equations, as well as the boundary conditions.

$$\eta = \sqrt{\frac{a}{\nu}}y, \quad \psi(\eta) = \sqrt{a\nu}xf$$

$$u = axf_\eta, \quad v = -\sqrt{a\nu}f$$

$$\theta = \frac{T - T_\infty}{T_w - T_\infty}, \quad \phi = \frac{C - C_\infty}{C_w - C_\infty}.$$

where η is the similarity variable, $\psi(\eta)$, $\theta(\eta)$ and $\phi(\eta)$ are stream, temperature and concentration functions respectively. By taking use of above similarity variables one can reduce equations (3.1)-(3.4) into the following nonlinear partial differential equations

$$\frac{\partial^2 f}{\partial \eta \partial \tau} - f\frac{\partial^2 f}{\partial \eta^2} - \frac{\partial^3 f}{\partial \eta^3} - (\frac{\partial f}{\partial \eta})^2 + (M + \frac{1}{Da})\frac{\partial f}{\partial \eta} - Gr\theta = 0, \tag{3.6}$$

$$Pr\frac{\partial \theta}{\partial \tau} + Pr(\theta\frac{\partial f}{\partial \eta} - f\frac{\partial \theta}{\partial \eta}) - (1 + Nr)\frac{\partial^2 \theta}{\partial \eta^2} - EcPr(\frac{\partial^2 f}{\partial \eta^2})^2$$
$$- EcPr(M + \frac{1}{Da})(\frac{\partial f}{\partial \eta})^2 - PrS\theta - PrNb\frac{\partial \theta}{\partial \eta}\frac{\partial \phi}{\partial \eta} - NtPr(\frac{\partial \theta}{\partial \eta})^2 = 0, \tag{3.7}$$

$$Le\frac{\partial \phi}{\partial \tau} + Le(\phi\frac{\partial f}{\partial \eta} - f\frac{\partial \phi}{\partial \eta}) - \frac{\partial^2 \phi}{\partial \eta^2} - \frac{Nt}{Nb}\frac{\partial^2 \theta}{\partial \eta^2} = 0, \tag{3.8}$$

here M, Pr, Nt, Nb, Da, Gr, Ec, S and Le are the magnetic parameter, Prandtl number, thermophoresis parameter, Brownian parameter, Darcy number, thermal Grashof

number, Eckert Number, heat source and Lewis number, respectively. These parameters are defined as [38]

$$Pr = \frac{\mu C_p}{k}, \quad M = \frac{\sigma B^2}{\rho a}, \quad Nt = \frac{\tau D_T (T_w - T_\infty)}{\nu T_\infty}, \quad Nb = \frac{\tau D_B (C_w - C_\infty)}{\nu},$$

$$Le = \frac{\nu}{D_B}, \quad Gr = \frac{\beta g b}{a^2}, \quad Da = \frac{Ka}{\nu}, \quad Ec = \frac{a u_w}{b C_p} \quad S = \frac{Q}{a \rho C_p}$$

After transformation the boundary conditions (3.5) take the form

$$(f_\eta, f, \theta, \phi) = (0, 0, 0, 0), \quad \text{at} \quad \tau = 0$$

$$(f_\eta, f, \theta, \phi) = (1 + \lambda f_{\eta\eta}, 0, 1, 1), \quad \text{at} \quad \eta = 0$$

$$(f_\eta, \theta) \to (0, 0), \quad \text{as} \quad \eta \to \infty \tag{3.9}$$

The skin friction coeffcient C_f is given by [24]

$$C_f = \frac{\tau_w}{\rho u_w^2}, \quad \text{where} \quad \tau_w = \mu u_y|_{y=0}, \tag{3.10}$$

the local Nusselt number Nu_x is given by [24]

$$Nu_x = \frac{x q_w}{k(T_w - T_\infty)}, \quad \text{where} \quad q_w = -k(1 + \frac{16 \sigma^* T_\infty^3}{3 k^* k}) T_y|_{y=0}, \tag{3.11}$$

and the local Sherwood number Sh_x is given by [32]

$$Sh_x = \frac{x j_w}{D(C_w - C_\infty)}, \quad \text{where} \quad j_w = -D C_y|_{y=0}. \tag{3.12}$$

After using the similarity transformations these equations (3.10), (3.11) and (3.12) becomes

$$\sqrt{Re_x} C_f = f_{\eta\eta}(0, \tau)$$

$$\frac{Nu_x}{\sqrt{Re_x}} = -(1 + Nr) T_\eta(0, \tau)$$

$$\frac{Sh_x}{\sqrt{Re_x}} = -\phi_\eta(0, \tau)$$

Here $Re_x = U x / \nu$ is a local Reynolds number.

22

3.3 Discretization

3.3.1 Spatial and Temporal Discretizations

We assume a domain $[0 \quad \eta_\infty] \times [0 \quad \tau_{end}]$ and $N+1$ grid points in the η-direction with equidistant grid spacing $\Delta\eta = \frac{\eta_\infty}{N}$ and τ_{end} is the end time with time step $\Delta\tau = \frac{\tau_{end}}{n_{end}}$. The coordinates of the grid points (i,n) are (η_i, τ_n) where $\eta_i = i\Delta\eta, i = 0, 1, ..., N$ and $\tau_n = n\Delta t, n = 0, 1, 2, ...$ The finite difference stencil is shown in Figure 2.1. For discretization in η-direction, we apply forward finite difference approximation for first order derivatives and central difference approximations for second order derivative. For time integration we use explicit Euler method. For implementation of FDM in MATLAB, we first reduce the order of a momentum equation by one. The order of unsteady temperature and concentration equations have not been reduced since it is already second order. All the finite difference approximation of all derivative is given below. Now we explain the procedure to reduce the order of the unsteady momentum equation. We assume $\frac{\partial f}{\partial \eta} = F$ then the Eqns (3.6)-(3.8) takes the following form:

$$\frac{\partial F}{\partial \tau} - f\frac{\partial F}{\partial \eta} - \frac{\partial^2 F}{\partial \eta^2} + (F)^2 + (M + \frac{1}{Da})F - Gr\theta = 0, \tag{3.13}$$

$$Pr\frac{\partial \theta}{\partial \tau} + Pr(\theta F - f\frac{\partial \theta}{\partial \eta}) - (1 + Nr)\frac{\partial^2 \theta}{\partial \eta^2} - EcPr(\frac{\partial F}{\partial \eta})^2 -$$
$$EcPr(M + \frac{1}{Da})(F)^2 - PrS\theta - PrNb\frac{\partial \theta}{\partial \eta}\frac{\partial \phi}{\partial \eta} - NtPr(\frac{\partial \theta}{\partial \eta})^2 = 0, \tag{3.14}$$

$$Le\frac{\partial \phi}{\partial \tau} + Le(\phi F - f\frac{\partial \phi}{\partial \eta}) - \frac{\partial^2 \phi}{\partial \eta^2} - \frac{Nt}{Nb}\frac{\partial^2 \theta}{\partial \eta^2} = 0, \tag{3.15}$$

The order of associated boundary conditions (3.9) reduces as follows:

$$(F, f, \theta, \phi) = (0, 0, 0, 0), \quad \text{at} \quad \tau = 0$$
$$(F, f, \theta, \phi) = (1 + \lambda F_\eta, 0, 1, 1), \quad \text{at} \quad \eta = 0$$
$$(F, \theta) \to (0, 0), \quad \text{as} \quad \eta \to \infty \tag{3.16}$$

To solve the above system of equations along with boundary conditions, we approximate the derivative appears in the partial differential equations (PDEs) by linear combinations of function values at the grid points by using the finite difference method (FDM). All the finite difference approximation of all orders are given by :

$$\left(\frac{\partial F}{\partial \eta}\right)_{(i,n)} = \frac{F_{i+1}^n - F_i^n}{\Delta \eta}, \quad \left(\frac{\partial^2 F}{\partial \eta^2}\right)_{(i,n)} = \frac{F_{i+1}^n - 2F_i^n + F_{i-1}^n}{(\Delta \eta)^2}, \quad \left(\frac{\partial F}{\partial \tau}\right)_{(i,n)} = \frac{F_i^{n+1} - F_i^n}{\Delta \tau},$$

$$\left(\frac{\partial \theta}{\partial \eta}\right)_{(i,n)} = \frac{\theta_{i+1}^n - \theta_i^n}{\Delta \eta}, \quad \left(\frac{\partial^2 \theta}{\partial \eta^2}\right)_{(i,n)} = \frac{\theta_{i+1}^n - 2\theta_i^n + \theta_{i-1}^n}{(\Delta \eta)^2}, \quad \left(\frac{\partial \theta}{\partial \tau}\right)_{(i,n)} = \frac{\theta_i^{n+1} - \theta_i^n}{\Delta \tau}$$

$$\left(\frac{\partial \phi}{\partial \eta}\right)_{(i,n)} = \frac{\phi_{i+1}^n - \phi_i^n}{\Delta \eta}, \left(\frac{\partial^2 \phi}{\partial \eta^2}\right)_{(i,n)} = \frac{\phi_{i+1}^n - 2\phi_i^n + \phi_{i-1}^n}{(\Delta \eta)^2}, \quad \left(\frac{\partial \phi}{\partial \tau}\right)_{(i,n)} = \frac{\phi_i^{n+1} - \phi_i^n}{\Delta \tau}$$

Here superscript 'n' and 'n+1' denotes the solution at n^{th} and $(n+1)^{th}$ time levels. And i, $i-1$ and $i+1$ is the location of the solution at current, previous and forward locations. Inserting all these approximation into the above equations Eqs. (3.13), (3.14) and (3.15).

$$\frac{F_i^{n+1} - F_i^n}{\Delta \tau} - \frac{F_{i+1}^n - 2F_i^n + F_{i-1}^n}{(\Delta \eta)^2} - f_i^n \frac{F_{i+1}^n - F_i^n}{\Delta \eta} + (F^n)^2 + (M + \frac{1}{Da})\frac{F_{i+1}^n - F_i^n}{\Delta \eta} - Gr\theta_i^n = 0,$$

$$Pr\frac{\theta_i^{n+1} - \theta_i^n}{\Delta \tau} + Pr\theta_i^n F_i^n - Prf_i^n(\frac{\theta_{i+1}^n - \theta_i^n}{\Delta \eta}) - (1 + Nr)\frac{\theta_{i+1}^n - 2\theta_i^n + \theta_{i-1}^n}{(\Delta \eta)^2} - EcPr(\frac{F_{i+1}^n - F_i^n}{\Delta \eta})^2$$

$$-EcPr(M + \frac{1}{Da})(F_i^n)^2 - PrS\theta_i^n - PrNb(\frac{\theta_{i+1}^n - \theta_i^n}{\Delta \eta})(\frac{\phi_{i+1}^n - \phi_i^n}{\Delta \eta}) - NtPr(\frac{\theta_{i+1}^n - \theta_i^n}{\Delta \eta})^2 = 0,$$

$$Le\frac{\phi_i^{n+1} - \phi_i^n}{\Delta \tau} + Le(\phi_i^n F_i^n - f_i^n \frac{\phi_{i+1}^n - \phi_i^n}{\Delta \eta}) - \frac{\phi_{i+1}^n - 2\phi_i^n + \phi_{i-1}^n}{(\Delta \eta)^2} - \frac{Nt}{Nb}\frac{\theta_{i+1}^n - 2\theta_i^n + \theta_{i-1}^n}{(\Delta \eta)^2} = 0.$$

The involved conditions reads as

$$\tau = 0: \quad F_i^0 = 0, \quad f_i^0 = 0, \quad \theta_i^0 = 0, \quad \phi_i^0 = 0$$

$$\eta = 0: \quad F_0^n = 1 + \lambda \frac{F_0^n - 2F_0^n + F_0^n}{(\Delta \eta)}, f_0^n = 0, \quad \theta_0^n = 1, \quad \phi_0^n = 1$$

$$\eta \to \infty: \quad F_{\eta_\infty}^n = 0, \quad \theta_{\eta_\infty}^n = 0, \quad \phi_{\eta_\infty}^n = 0$$

The important parameters for finite difference implementation read as:

local Nusselt Number:

$$\frac{Nu_x}{\sqrt{Re_x}} = -(1 + Nr)\frac{\theta_1^n - \theta_0^n}{\Delta \eta}.$$

local Sherwood Number:

$$\frac{Sh_x}{\sqrt{Re_x}} = -\frac{\phi_1^n - \phi_0^n}{\Delta \eta}.$$

Skin Friction Coefficient

$$\sqrt{Re_x}C_f = \frac{F_1^n - F_0^n}{(\Delta \eta)}.$$

3.4 Results and Discussion

Here we present the graphical results of velocity and temperature have been presented. Variations of Gr, M, Nt has been focused specifically. Figure 3.1 (a) and (b) elucidate the effects of τ on velocity profile under the influence of thermophoresis as well as magnetic parameter. To illustrate our findings we present results graphically. A noticeable increasing behavior in velocity profiles has been observed here.

The influence of unsteady parameter on temperature and thermal boundery layer thickness is similar to that of velocity as shown in Figure 3.2 (a) and (b). It is evident that the larger value of Nt dampen the temperature value in 3.2 (a). However, Figure 3.2 (b) professes an increase in temperature near the boundary for the value of M or without M.

Figure 3.3 speaks about the effect of Gr on concentration profile with an increase of Da. Gr has a huge impact on concentration profile. However, we see a hairline change in concentration profile in Figure 3.3 (b) with and without M.

Finally, in Figure 3.4 we witness the effect of Da on a temperature profile with and without Gr. It depicts that without the presence of Gr the temperature is higher near the surface compare with the presence of the higher values of Gr.
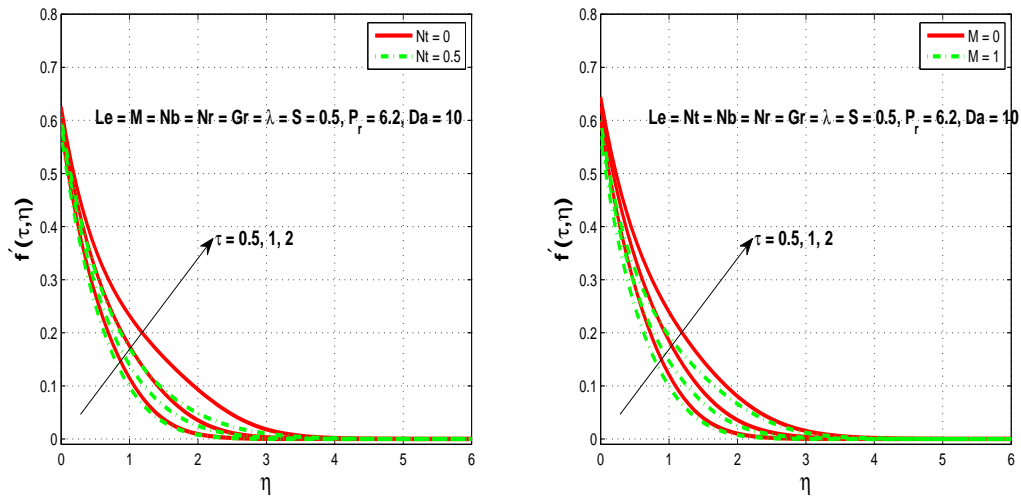
Figure 3.1: Computational velocity profiles against variation values of Nt and M.
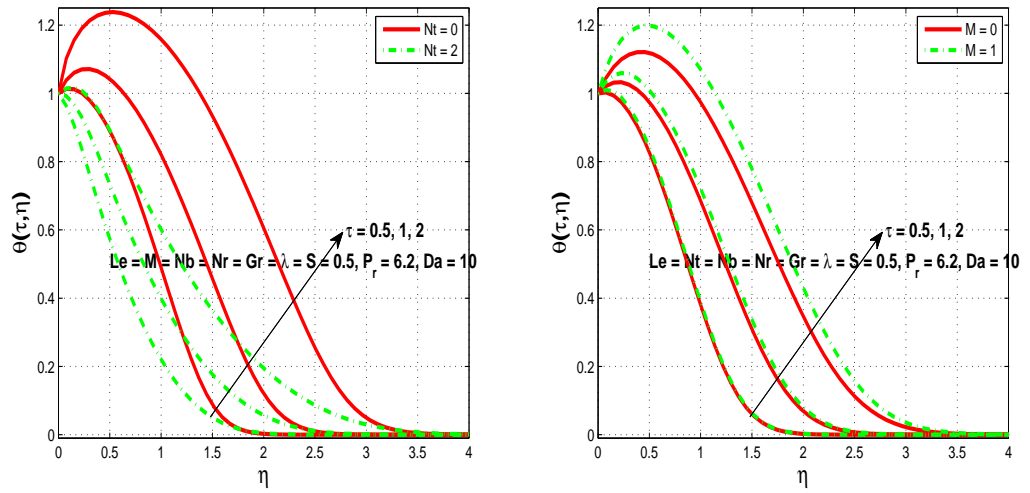
Figure 3.2: Computational temperature against variable values of Nt and M.
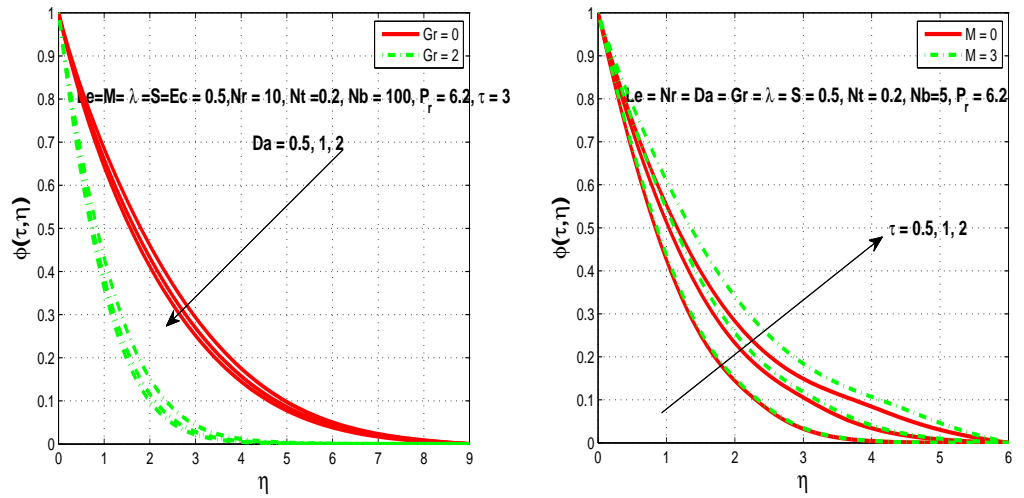
Figure 3.3: Computational concentration profile against variation of different paramters.
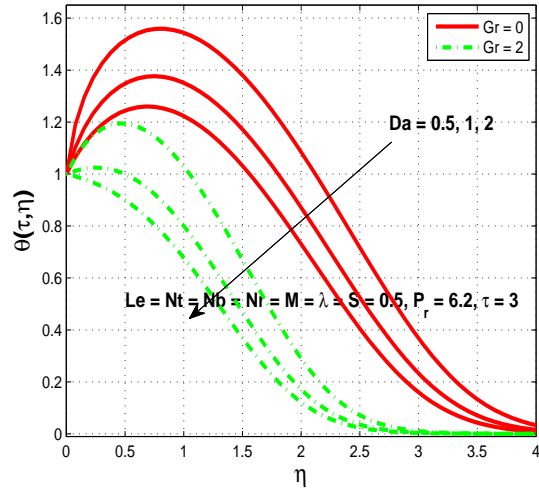
Figure 3.4: Computational temperature against variable values of Gr.

Chapter 4

Simplified FDM for nanofluid Flow above an Exponentially Stretching Surface Submerged in a Permeable Medium

In this chapter we develop a numerical method as an elaborate inquiry apply to steady nanofluid flow past in a Magnetic field past an exponentially stretchable surface. The developed numerical technique is the simplified FDM which uses LU-Factorization. The simplified FDM is useful in computing numerical solution for a general class of coupled ODEs. We show that the simplified FDM remarkably gives good results when compare with *bvp4c* and results from literature.

The chapter is planned in the following order: Section 4.1 commences by laying out the mathematical model of the physical problem. Section 4.2 is devoted to develop methodology. Numerical procedure is opted and discussed in Section 4.3. In the same section the detailed description of the simplified FDM is given. As a consequence of numerical calculations Results and Discussion is followed in Section 4.4.

4.1 Mathematical Formulation

We deliberate a 2-D, steady, incompressible, MHD, laminar nanofluid flow occupied over a slippery surface in a permeable medium. After making these assumptions, the governing equations consisting of continuity, momentum, energy and concentration can be constructed in the following forms by valuing the Buongiorno model concept [45] :

$$\partial_x u + \partial_y v = 0, \tag{4.1}$$

$$u u_x + v u_y = \nu u_{yy} - \frac{\sigma B_o^2 u}{\rho} - \frac{\nu u}{K} + g\beta(T - T_\infty), \tag{4.2}$$

$$u T_x + v T_y = \frac{k}{\rho C_p}(T_{yy}) + \frac{\nu}{C_p}(u_y)^2 + \frac{\sigma B_o^2 u^2}{\rho C_p} + \frac{\nu u^2}{C_p K} - \frac{1}{\rho C_p} q_{r,y} + \frac{Q(T - T_\infty)}{\rho C_p}$$
$$+ \tau[D_B(C_y T_y) + \frac{D_T}{T_\infty}(T_y)^2], \tag{4.3}$$

$$u C_x + v C_y = D_B(C_{yy}) + \frac{D_T}{T_\infty}(T_{yy}), \tag{4.4}$$

where u and v are the velocity components direction parallel to surface and normal to it, respectively. μ is the coefficient of viscosity, ρ is the density of the fluid, σ is the electrical conductivity of the fluid, T is fluid's temperature, K is the permeability, β is the thermal expansion coefficient, k is usually refer as the thermal conductivity, C_p refers the specific heat, q_r is the radioactive heat flux, Q is the heat source coefficient, C is the concentration, $\tau = (\rho C)_p/(\rho C)_f$, here $(\rho C)_p$ and $(\rho C)_f$ are heat capacities of the nanofluid and base fluid, respectively. Also D_B , D_T are Brownian and thermophoretic diffusion coefficients, respectively. The ambient fluid temperature is regarded as T_∞ and the ambient fluid concentration is regarded as C_∞.

4.1.1 Boundary Conditions

The preceding mathematical model allow the following boundary condition:

$$(u, v, T, C) = (U_w + \frac{\mu}{L_1} u_y, 0, T_w, C_w), \quad at \quad y = 0 \tag{4.5}$$
$$(u, T, C) \to (0, T_\infty, C_\infty) \quad as \quad y \to \infty$$

30

where L_1 is the slip length.

Also

- $U_w = U_0 exp\left(\frac{x}{L}\right)$

- $T_w = T_\infty + T_0 exp\left(\frac{x}{2L}\right)$

- $C_w = C_\infty + C_0 exp\left(\frac{x}{2L}\right)$

4.2 Method of Solution

We apply following similarity parameters for the momentum, energy and concentration equations (4.1)-(4.4) as well as for the boundary conditions (4.5).

$$\eta_\eta = \sqrt{\frac{U_0}{2\nu L}}e^{x/(2L)}y, \quad \psi(\eta) = \sqrt{2U_0\nu L}e^{x/(2L)}f$$

$$u = U_0 f'e^{x/L}, \quad v = -\sqrt{\frac{U_0\nu}{2L}}e^{x/(2L)}(f'\eta_\eta + f)$$

$$\theta = \frac{T - T_\infty}{T_0}e^{-x/(2L)}, \quad \phi = \frac{C - C_\infty}{C_0}e^{-x/(2L)},$$

In above equations η is the similarity variable, (ψ, θ, ϕ) are stream function, temperature and concentration, respectively.

$$f''' + ff'' - 2(f')^2 - (M_f + \frac{1}{Da})f' + 2Gr\theta = 0, \qquad (4.6)$$

$$Pr(\theta f' - f\theta') - (1+Nr)\theta'' - PrEc(f'')^2 - PrEc(M_f + \frac{1}{Da})(f')^2 - 2PrS\theta - PrNb\phi'\theta' - PrNt\theta'^2 = 0, \qquad (4.7)$$

$$\phi'' + \frac{Nt}{Nb}\theta'' + Le(f\phi' - f'\phi) = 0, \qquad (4.8)$$

31

here M_f, Pr, Nt, Nb, Gr, Da, Nr, Ec, S, and Le are the magnetic parameter, Prandtl number, thermophoresis parameter, Brownian parameter, Grashof number, Darcy's number, thermal radiation effect, heat source or sink and Lewis number, respectively. These are defined as

$$Pr = \frac{\mu C_p}{k}, \quad M_f = \frac{2L\sigma B_0^2}{U_w \rho}, \quad Nt = \frac{\tau D_T (T_w - T_\infty)}{T_\infty \nu}, \quad Nb = \frac{\tau D_B (C_w - C_\infty)}{\nu}, \quad Le = \frac{\nu}{D_B},$$

$$Gr = \frac{\beta g L (T_w - T_\infty)}{U_w^2}, \quad Da = \frac{K U_w}{2\nu L}, \quad Ec = \frac{U_w^2}{T_w C_p}, \quad S = \frac{QL}{U_w \rho C_p}.$$

After transformation the boundary conditions (4.5) takes the form

$$\eta_\eta = 0: \quad (f, f', \theta, \phi) = (0, 1 + \lambda f'', 1, 1),$$

$$\eta_\eta = \infty: \quad (f', \theta, \phi) \rightarrow (0, 0, 0), \tag{4.9}$$

in above the slip parameter is signified by λ.

The skin friction coefficient C_f is given by [36]

$$C_f = \frac{\nu}{u_w^2} \left(\frac{\partial u}{\partial y} \right)_{y=0}. \tag{4.10}$$

The local Nusselt number Nu_x is written as [36]

$$Nu_x = -(1 + Nr) \frac{x}{(T_w - T_\infty)} \left(\frac{\partial T}{\partial y} \right)_{y=0}. \tag{4.11}$$

For concentration additional quantity.

local Sherwood number Sh_x can be defined as [36]

$$Sh_x = -\frac{x}{(C_w - C_\infty)} \left(\frac{\partial C}{\partial y} \right)_{y=0}. \tag{4.12}$$

After using the similarity transformations these equations (4.10), (4.11) and (4.12) becomes

$$C_f = \frac{1}{\sqrt{2Re_x}} f''(0)$$

$$Nu_x = -(1 + Nr) \sqrt{\frac{x Re_x}{2L}} \theta'(0)$$

$$Sh_x = -\sqrt{\frac{x Re_x}{2L}} \phi'(0)$$

Here $Re_x = Ux/\nu$ is a local Reynolds number .

4.3   Numerical Procedures

In search of solution for the above problem given in (4.6)-(4.8) the only plausible way is to compute answers numerically. We attempt to find numerical solutions by two numerical techniques. The first one is the simplified FDM and second is the famous numerical algorithm written in MATLAB and commonly known by *bvp4c*. Therefore, due details on the simplified FDM will be presented first followed by some brief description about *bvp4c*.

4.3.1   Simplified FDM

This work is inspired from Na [46] where some fancy results are presented for scalar boundary values problems. We extend these concepts for the coupled nonlinear ODEs and implement these in MATLAB. The algorithm with necessary details for the simplified FDM are as follows:

1. We first exercise to reduce the third order ODE into a group of first and second order ODEs. This necessarily means to simplify the process of finite difference approximation.

2. To further simplify, we use Taylor series to linearize the system of nonlinear ODEs.

3. We immediately replace the derivatives in linear ODEs with the corresponding finite difference approximation formulas.

4. Eventually, we reach at algebraic system of equations that can be solved efficiently by LU-decomposition.

We establish the results for $N = 1000$ grid points in the η direction. Generally, the domain to achieve steady state varies due to influence of different parameters, however,

the domain $\eta = 7$ seems enough for our results. To initiate reduction preceding, we assume $f' = F$ in (4.6) then we get

$$\frac{d^2 F}{d\eta_\eta^2} = -f\frac{dF}{d\eta_\eta} + 2F^2 + (M_f + \frac{1}{Da})F - 2Gr\theta, \tag{4.13}$$

we can write this expression for the function ϕ_1 as

$$\phi_1(\eta_\eta, F, F') = -f\frac{dF}{d\eta_\eta} + 2F^2 + (M_f + \frac{1}{Da})F - 2Gr\theta, \tag{4.14}$$

let us approximate $\frac{dF}{d\eta_\eta}$ in above equation by forward difference approximation

$$\phi_1(\eta_\eta, F, F') = -f_i(\frac{F_{i+1} - F_i}{d\eta_\eta}) + 2F_i^2 + (M_f + \frac{1}{Da})F_i - 2Gr\theta_i. \tag{4.15}$$

$$\psi_1(\eta_\eta, F, F', f'') = \frac{d^2 F}{d\eta_\eta^2} - \phi_1(\eta_\eta, F, F') = 0 \tag{4.16}$$

The coefficients of second order ODE read as

$$A_n = -\frac{\partial \phi_1}{\partial F'} = -(-f) = f = f_i \tag{4.17}$$

$$B_n = -\frac{\partial \phi_1}{\partial F} = -4F - (M_f + \frac{1}{Da}) \tag{4.18}$$

$$B_n = -4F_i - (M_f + 1/Da) \tag{4.19}$$

$$D_n = \phi_1(\eta_\eta, F, F') + B_n F_i + A_n \frac{F_{i+1} - F_i}{d\eta_\eta} \tag{4.20}$$

After some manipulation (4.15) becomes

$$a_i F_{i-1} + b_i F_i + c_i F_{i+1} = r_i, \qquad i = 1, 2, 3...., N \tag{4.21}$$

where

$$a_i = 2 - hA_n, \qquad b_i = 2h^2 B_n - 4, \qquad c_i = 2 + hA_n, \qquad r_i = 2h^2 D_n \tag{4.22}$$

34

In matrix-vector form it is written in compact as

$$AF = s \tag{4.23}$$

where

$$A = \begin{bmatrix} b_1 & c_1 & & & & \\ a_2 & b_2 & c_2 & & & \\ & & .... & & & \\ & & & a_{N-2} & b_{N-2} & c_{N-2} \\ & & & & a_{N-1} & b_{N-1} \end{bmatrix} \tag{4.24}$$

$$F = \begin{bmatrix} F_1 \\ F_2 \\ . \\ . \\ F_{N-1} \end{bmatrix} \qquad s = \begin{bmatrix} s_1 \\ s_2 \\ . \\ . \\ s_{N-1} \end{bmatrix} \tag{4.25}$$

The matrix A is tridiagonal matrix and is written in LU-Factorization as

$$A = LU \tag{4.26}$$

where

$$L = \begin{bmatrix} \beta_1 & & & & \\ a_2 & \beta_2 & & & \\ & & .... & & \\ & & a_{N-2} & \beta_{N-2} & \\ & & & a_{N-1} & \beta_{N-1} \end{bmatrix} \tag{4.27}$$

and

$$U = \begin{bmatrix} 1 & \gamma_1 & & & \\ & 1 & \gamma_2 & & \\ & & .... & & \\ & & & 1 & \gamma_{N-2} \\ & & & & 1 \end{bmatrix} \tag{4.28}$$

where L and U are the lower and upper triangular matrices, respectively. Here (β_i, γ_i) $(i = 1, 2, ..., N - 1)$ has to be discovered which are related by

$$\beta_1 = -1 - \frac{\lambda}{h}, \qquad \gamma_1 = \frac{\lambda}{\beta_1 h} \tag{4.29}$$

35

$$\beta_i = b_i - a_i \gamma_{i-1}, \quad i = 2, 3, ..., N-1 \tag{4.30}$$

$$\beta_i \gamma_i = c_i, \quad i = 2, 3, ..., N-2 \tag{4.31}$$

After defining these relations (4.23) becomes

$$LUF = s, \quad UF = z, \quad \text{and} \quad Lz = s \tag{4.32}$$

we have

$$
\begin{bmatrix}
\beta_1 & & & & \\
a_2 & \beta_2 & & & \\
& & .... & & \\
& & a_{N-2} & \beta_{N-2} & \\
& & & a_{N-1} & \beta_{N-1}
\end{bmatrix}
\begin{bmatrix}
z_1 \\
z_2 \\
z_3 \\
. \\
. \\
. \\
z_{N-2} \\
z_{N-1}
\end{bmatrix}
=
\begin{bmatrix}
s_1 \\
s_2 \\
s_3 \\
. \\
. \\
. \\
s_{N-2} \\
s_{N-1}
\end{bmatrix}
\tag{4.33}
$$

The unknown elements of z can be found by

$$z_1 = s_1/\beta_1, z_i = \frac{s_i - a_i z_{i-1}}{\beta_i}, i = 2, 3, ..., N-1 \tag{4.34}$$

and

$$
\begin{bmatrix}
1 & \gamma_1 & & & \\
& 1 & \gamma_2 & & \\
& & .... & & \\
& & & 1 & \gamma_{N-2} \\
& & & & 1
\end{bmatrix}
\begin{bmatrix}
F_1 \\
F_2 \\
. \\
. \\
. \\
F_{N-2} \\
F_{N-1}
\end{bmatrix}
=
\begin{bmatrix}
z_1 \\
z_2 \\
. \\
. \\
. \\
z_{N-2} \\
z_{N-1}
\end{bmatrix}
\tag{4.35}
$$

We then get

$$F_{i-1} = z_{i-1}, \quad F_i = z_i - \gamma_i F_{i+1}, \quad i = N-2, N-3, ..., 3, 2, 1 \tag{4.36}$$

which is a solution of (4.13). We can easily find f from $f' = F$ which in discretization form is written as

$$\frac{f_{i+1} - f_i}{d\eta_\eta} = F_i \tag{4.37}$$

gives a required solution of (4.6). A similar procedure can also opted for solutions θ and ϕ. For the sake of brevity, we only present coefficients for these ODEs and leave the details which follows on the same line as presented above. For example, we have energy and concentration equations as

$$\frac{d^2\theta}{d\eta_\eta^2} = \frac{1}{1 + N_r}\left\{ Pr\left(\theta F - f\frac{d\theta}{d\eta_\eta}\right) - PrEc(\frac{dF}{d\eta_\eta})^2 - PrEc(M_f + \frac{1}{Da})F^2 \right\}$$
$$- \frac{1}{1 + N_r}\left\{ 2PrS\theta - PrNb\frac{d\phi}{d\eta_\eta}\frac{d\theta}{d\eta_\eta} - PrNt\left(\frac{d\theta}{d\eta_\eta}\right)^2 \right\} \tag{4.38}$$

$$\phi_2(\eta_\eta, \theta, \theta') = \frac{1}{1 + N_r}\left\{ Pr\left(\theta_i F_i - f_i\frac{\theta_i - \theta_{i-1}}{d\eta_\eta}\right) - PrEc(\frac{F_i - F_{i-1}}{d\eta_\eta})^2 - PrEc(M_f + \frac{1}{Da})F_i^2 \right\}$$
$$- \frac{1}{1 + N_r}\left\{ PrNb\frac{\phi_i - \phi_{i-1}}{d\eta_\eta}\frac{\theta_i - \theta_{i-1}}{d\eta_\eta} - PrNt\left(\frac{\theta_i - \theta_{i-1}}{d\eta_\eta}\right)^2 - 2PrS\theta_i \right\} \tag{4.39}$$

$$A_{nn} = -\frac{\partial\phi_2}{\partial\theta'} = -\frac{1}{1 + N_r}\left\{ -Prf - PrNb\frac{d\phi}{d\eta_\eta} - 2PrNt\frac{d\theta}{d\eta_\eta} \right\} \tag{4.40}$$

$$A_{nn} = -\frac{\partial\phi_2}{\partial\theta'} = \frac{1}{1 + N_r}\left\{ Prf_i + PrNb\frac{d\phi_i - \phi_{i-1}}{d\eta_\eta} + 2PrNt\frac{d\theta_i - \theta_{i-1}}{d\eta_\eta} \right\} \tag{4.41}$$

$$B_{nn} = -\frac{\partial\phi_2}{\partial\theta} = \frac{-1}{1 + N_r}\left\{ PrF - 2PrS \right\} \tag{4.42}$$

$$B_{nn} = -\frac{\partial\phi_2}{\partial\theta} = \frac{-1}{1 + N_r}\left\{ PrF_i - 2PrS \right\} \tag{4.43}$$

$$\frac{d^2\phi}{d\eta_\eta^2} = \frac{-Nt}{Nb}\frac{d^2\theta}{d\eta_\eta^2} - Le\left(f\frac{d\phi}{d\eta_\eta} - F\phi\right) \tag{4.44}$$

$$\phi_3(\eta_\eta, \phi, \phi') = \frac{-Nt}{Nb}\frac{\theta_{i-1} - 2\theta_i + \theta_{i+1}}{d\eta_\eta^2} - Le\left(f_i\frac{\phi_i - \phi_{i-1}}{d\eta_\eta} - F_i\phi_i\right) \tag{4.45}$$

Similarly, the coefficeints for (4.8) are written as

$$A_{nnn} = Lef_i, \qquad B_{nnn} = -LeF_i \tag{4.46}$$

Boundary condition are discretized as

$$F_1 = 1 + \lambda\left(\frac{F_2 - F_1}{d\eta_\eta}\right) \tag{4.47}$$

where $dh \approx \Delta\eta_\eta$

4.3.2 $bvp4c$

In order to solve the system of equations (4.6)-(4.8) along with boundary conditions (4.9)) we use a MATLAB built-in function bvp4c. Description of the method can be seen in [47]. We define the variables as

$$y_1 = f, \quad y_2 = f', \quad y_3 = f'', \quad y_4 = \theta, \quad y_5 = \theta' \quad y_6 = \phi, \quad y_7 = \phi' \tag{4.48}$$

The system of first order equations is given below

$$y_1' = f' = y_2, \tag{4.49}$$

$$y_2' = f'' = y_3, \tag{4.50}$$

$$y_3' = f''' = -y_1y_3 + 2(y_2)^2 + \left(M_f + \frac{1}{Da}\right)y_2 - 2Gry_4, \tag{4.51}$$

$$y_4' = \theta' = y_5, \tag{4.52}$$

$$y_5' = \theta'' = \frac{1}{1 + Nr}(Pry_4y_2 - Pry_1y_5 - PrEcy_3^2 - \left(M_f + \frac{1}{Da}\right)EcPry_2^2$$
$$-2PrSy_4 - PrNby_7y_5 - NtPry_5^2), \tag{4.53}$$

38

$$y_6' = \phi' = y_7, \tag{4.54}$$

$$y_7' = \phi'' = Le y_6 y_2 - Le y_1 y_7 - \frac{Nt}{Nb} y_5', \tag{4.55}$$

and boundary conditions are given as

$$y_0(1) = 0, \quad y_0(2) - 1 - \lambda y_0(3) = 0, \quad y_0(4) - 1 = 0, \quad y_0(6) - 1 = 0 \tag{4.56}$$

$$y_{inf}(2) = 0, \quad y_{inf}(4) = 0, \quad y_{inf}(6) = 0$$

4.4   Results and Discussion

In this section, we give results in quantitative as well as qualitative form.

First of all, we compare our findings of $f''(0)$ with those of previously published paper as shown in Table 1. Both results are found in close agreement with each other.

From Table 2, one can observe that the skin friction coefficient increases while there is a reduction in both wall temperature and concentration gradients as we raise the magnetic parameter. We also observed that the magnitude of local Nusselt number and local Sherwood number increases and the skin friction coefficient decreases as we raise the values of Darcy's number. Grashof number enhances local Nusselt number and local Sherwood number whereas it reduces the skin friction coefficient. Furthermore , Lewis number Le causes slight change in the skin friction coefficient while concentration gradient increases and wall temperature gradient reduces.

Roughness of wall, local heat flux and concentration flux at wall decreases as increasing the values of thermophoretic parameter Nb as visible in Table 3. It is also evident from the Table 2 that local Sherwood number increases by increasing Nt but the effect is seen to be reverse on the skin friction coefficient while local Nusselt number remains constant. From Table 3 one can also see the effect of Ec causes an increase in local Sherwood number whereas the effect is opposite on the skin friction coefficient and local Nusselt number.

Table 4.1: The comparison of skin friction coefficient $(-f''(0))$ to previous data for $\lambda = S = Ec = Nr = Gr = 0$, $Da = \infty$ and for various vales Pr, M, Nb, Nt and Le.

Pr	M_f	Nb	Nt	Le	Sharif et al. [48]	bvp4c	Simplified FDM
0.7	0	0.5	0.5	1	1.28183	1.2818089	1.2646694
-	0.1	-	-	-	1.32104	1.3210148	1.3030810
-	0.2	-	-	-	1.35895	1.3589575	1.3402296
-	0.3	-	-	-	1.39581	1.3957745	1.3762525

Table 4.2: Results for $-f''(0)$, $-\theta'(0)$ and $-\phi'(0)$ obtained by fixing values of parameters $Pr = 6.2$, $Nt = 2$, $Ec = 0.2$, $Nb = 8$, $S = 0.1$, $Nr = 5$ and $\lambda = 3$.

				bvp4c			Simplified FDM		
M	Da	Gr	Le	$-f''(0)$	$-\theta'(0)$	$-\phi'(0)$	$-f''(0)$	$-\theta'(0)$	$-\phi'(0)$
1	4	0.3	8	0.1945	0.0100	2.2070	0.1945175	0.0099219	2.196740
1.1	-	-	-	0.1977	0.0094	2.1769	0.1977045	0.0093481	2.1669909
1.2	-	-	-	0.2008	0.0088	2.1477	0.2007573	0.0087879	2.1380916
1.3	-	-	-	0.2037	0.0083	2.1193	0.2036818	0.0082440	2.1100172
1	5	0.3	8	0.1929	0.0103	2.2223	0.1928713	0.0102230	2.2119414
-	6	-	-	0.1918	0.0105	2.2327	0.1917538	0.010423	2.2221985
-	7	-	-	0.1910	0.0106	2.2401	0.1909458	0.0105674	2.2295847
-	8	-	-	0.1903	0.0107	2.2458	0.1903340	0.0106763	2.2351598
1	5	0.4	8	0.1754	0.0121	2.3805	0.1753267	0.0121091	2.3689312
-	-	0.5	-	0.1592	0.0136	2.5161	0.1591568	0.0136077	2.5033457
-	-	0.6	-	0.1441	0.0149	2.6354	0.1440571	0.0148417	2.6216478
-	-	0.7	-	0.1299	0.0159	2.7426	0.1298239	0.0158828	2.7277798
1	5	0.7	9	0.1302	0.0159	2.9079	0.1301768	0.0149605	2.8912397
-	-	-	13	0.1313	0.0124	3.4900	0.1312932	0.0124113	3.4660959
-	-	-	17	0.1321	0.0108	3.9863	0.1321069	0.0108305	3.9552333
-	-	-	21	0.1328	0.0097	4.4263	0.1327388	0.0097292	4.3880280

Table 4.3: Results for $-f''(0)$, $-\theta'(0)$ and $-\phi'(0)$ obtained by various values of parameters $Pr = 6.2$, $M_f = 2$, $Da = 5$, $Gr = 0.7$, $Nr = 5$, $Le = 8$ and $\lambda = 3$.

Nb	Nt	Ec	bvp4c			Simplified FDM		
			$-f''(0)$	$-\theta'(0)$	$-\phi'(0)$	$-f''(0)$	$-\theta'(0)$	$-\phi'(0)$
2	2	0.2	0.1660	0.0270	2.4876	0.1682158	0.0746442	2.4973830
6	-	-	0.1648	0.0148	2.4800	0.1647564	0.0148202	2.4679691
8	-	-	0.1641	0.0104	2.4777	0.1640238	0.0104038	2.4656461
10	-	-	0.1636	0.0081	2.4774	0.1635227	0.0081378	2.4652570
10	0.5	0.1	0.1656	0.0106	2.4477	0.1655962	0.0105904	2.4350691
-	1	-	0.1650	0.0106	2.4580	0.1649419	0.0106063	2.4455417
-	1.5	-	0.1644	0.0106	2.4668	0.1643695	0.0106205	2.4546071
-	2	-	0.1639	0.0106	2.4745	0.163872	0.0106326	2.4624605
15	2	0	0.1634	0.0086	2.4739	0.1632997	0.0086251	2.4618319
-	-	0.1	0.1631	0.0070	2.4763	0.1630272	0.0069807	2.4641318
-	-	0.2	0.1628	0.0053	2.4787	0.1627443	0.0053296	2.4665070
-	-	0.3	0.1625	0.0037	2.4812	0.1624500	0.0036714	2.4689664

4.4.1 Effect of Magnetic Parameter M_f

Figure 4.1(a) shows velocity profile which decreases as M_f increases until $\eta \approx 2.50$ but afterwards boundary layer thickness demonstrate the opposite behaviorr. Figure 4.1 (b) we illustrate that the increase in thermal boundary layer thickness is due to an increase of magnetic parameter. But we observe minor increase in concentration profile presented in Figure 4.2(a). The physics behind reduction of momentum boundary layer is that with the increase in M_f, Lorentz force increase and it produces more resistance to flow but after certain values incremental M_f overcome Lorentz force.

4.4.2 Effects of Darcy Number Da

Darcy number commonly used in heat transfer through porous media. With increase of Darcy's number thermal boundary layer thickness decrease as presented in Figure 4.3(b). It is observed from Figures 4.2(b) and 4.3(a) that by increasing values of Darcy number velocity increases and concentration profile decreases but the effect.

4.4.3 Effects of Grashof Number Gr

Gr approximates the ratio of buoyancy to viscous forces and represent how dominant is buoyancy force which is responsible for the conviction comparing to viscous forces. These effect are displayed in Figures 4.4(b), 4.5(a) and 4.5(b). It can be observed that temperature and concentration decreases with Grashof number but there is abrupt change in velocity profile.

4.4.4 Effects of Lewis Number Le

Figure 4.4(a) demonstrate nanoparticle volume fraction for several values of Lewis number Le and accompanying reduction in its concentration boundary layer thickness. It is observed from the Figure 14.9(b) that temperature profile as well as thickness of boundary layer initially increases and then decreases with Lewis number. Figure 14.9(a) shows the variation of velocity profile with variation of Lewis number. It is observed that velocity profile decreases with increasing Le. This implies that momentum boundary layer thickness decreases when ratio of thermal diffusivity to mass diffusivity increases.

4.4.5 Effects of Nt

It is observed from Figure 4.7(a) that Nt increases the velocity profile with a marked increase in momentum boundary layer thickness. Figure 4.7(b) illustrates variation of temperature profile on thermophoretic parameter. It is validated the fact that the thermophoretic parameter enhances the temperature profile. Because thermophoretic phenomenon transferred nanoparticles form hot surface to the cold region which results in increase in temperature of the fluid. Figure 4.6(a) suggests that a stronger thermophoretic parameter produce minor change in nanoparticle volume fraction.

4.4.6 Effects of Nb

Figure 4.8(b) suggests that a stronger Brownian motion is responsible for an increase in thermal boundary layer thickness. Incremental Brownian parameter causes slight

change in nanoparticles volume fraction while increase in velocity profile as presented in Figures 4.6(b) and 4.8(a).

4.4.7 Effects of Eckert Number Ec

Eckert number plays an important role, in high speed flows for which viscous dissipation is significant. From Figures 4.10(a), 4.10(b) and 4.11 the effects of this dissipation on velocity, temperature and concentration profile have been shown. It depicts that without Ec the behavior of velocity at the surface is low then increase with Ec. The temperature is low inner part of the thermal boundary layer but high with Ec [Figure 4.10(b)] while the effect of viscous dissipation is insignificant on concentration profile as presented in Figure 4.11.

Pr = 6.2, Da = 5, Gr = 2, Nr = 5, Nb = 2, Nt = 0.5, Ec= 0.1, Le = 5,λ = 0.5, S = 0.1

Pr = 6.2, Da = 5, Gr = 2, Nr = 5, Nb = 2, Nt = 0.5, Ec= 0.1, Le = 5,λ = 3, S = 0.1
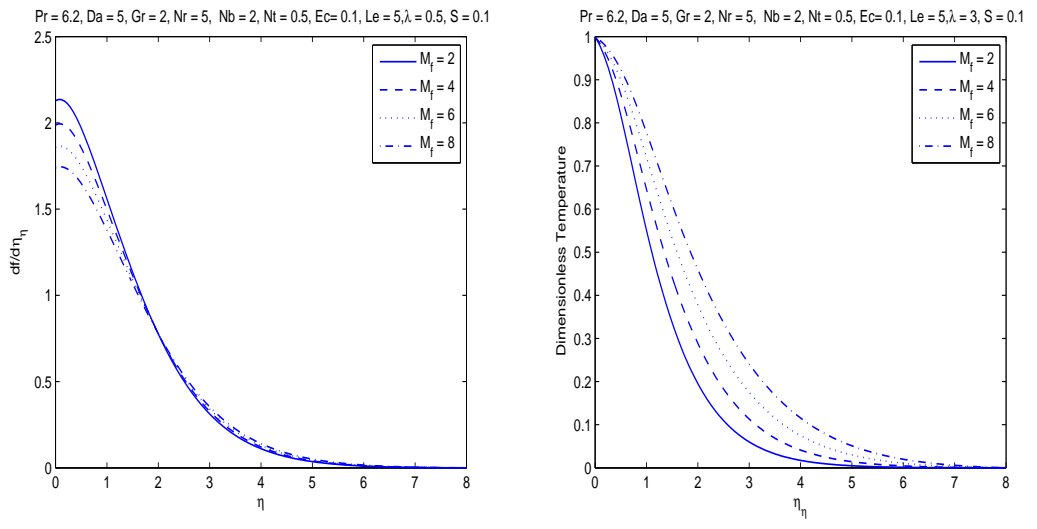
Figure 4.1: Computational velocity and temperature profiles against variation values of M_f.
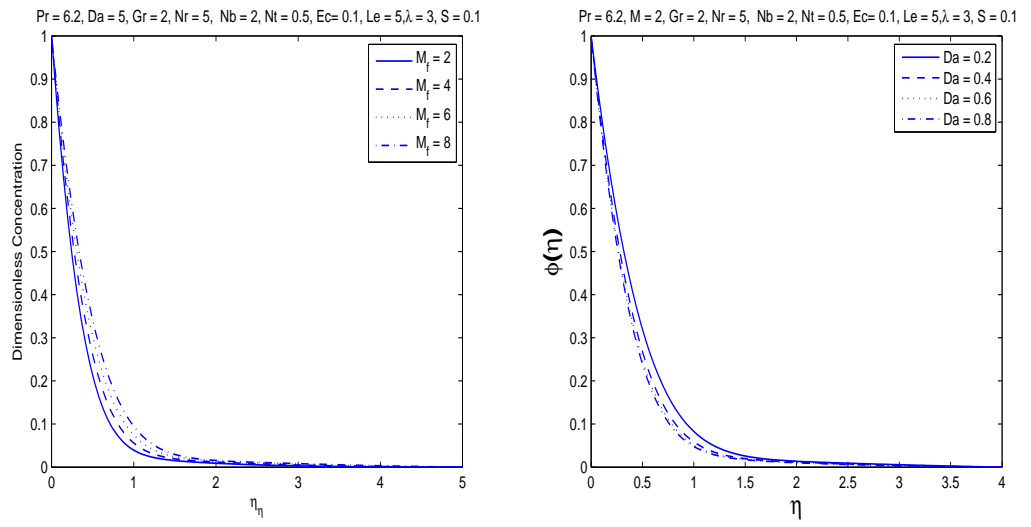
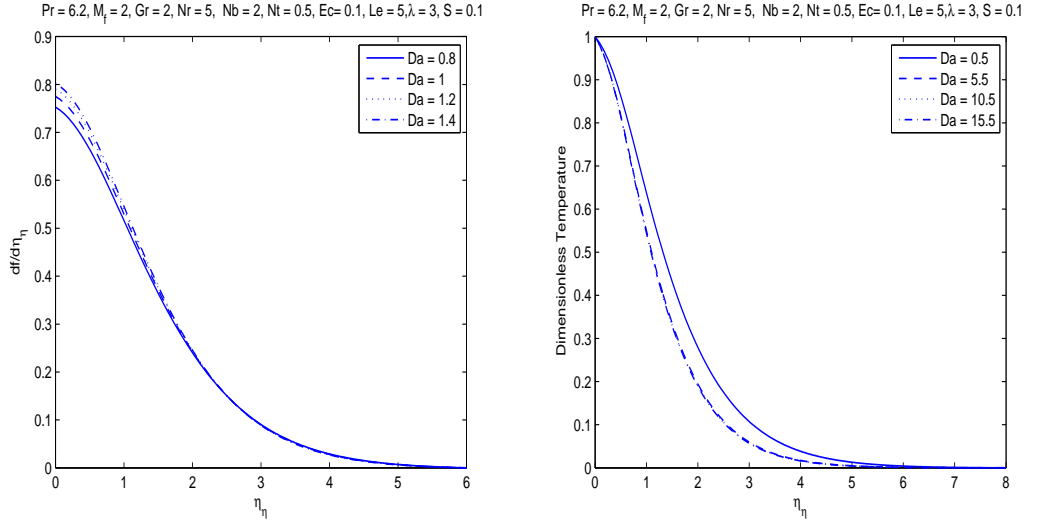Figure 4.2: Computational concentration profiles against variation values of M_f and Da.

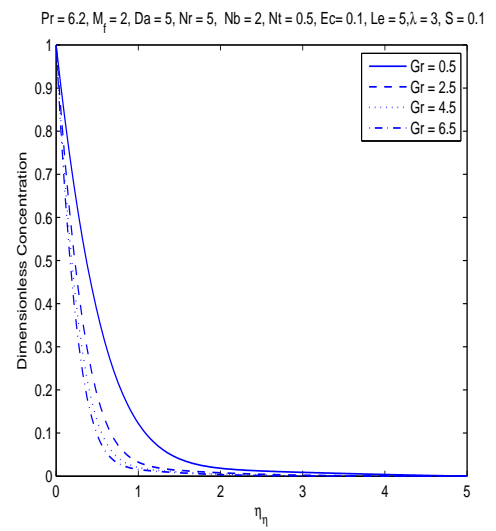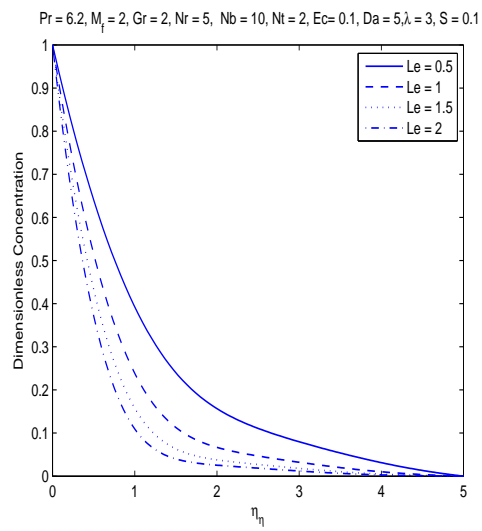Figure 4.3: Computational velocity and temperature profiles against variation values of Da.

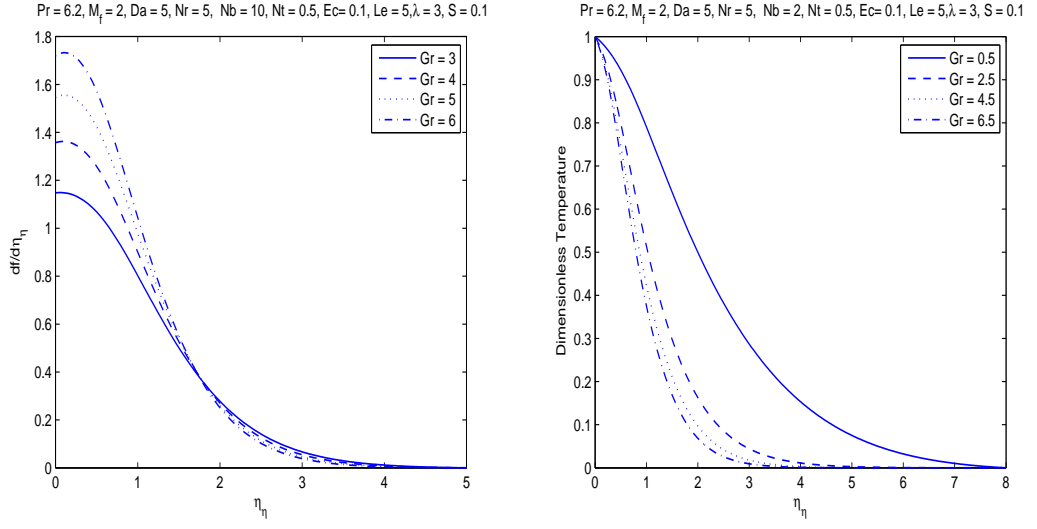Figure 4.4: Computational concentration profiles against variation values of Le and Gr.

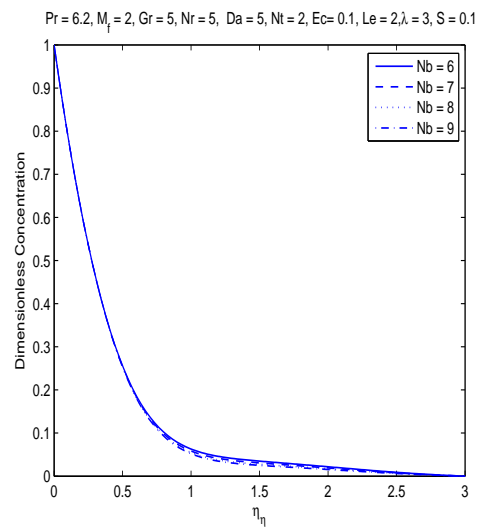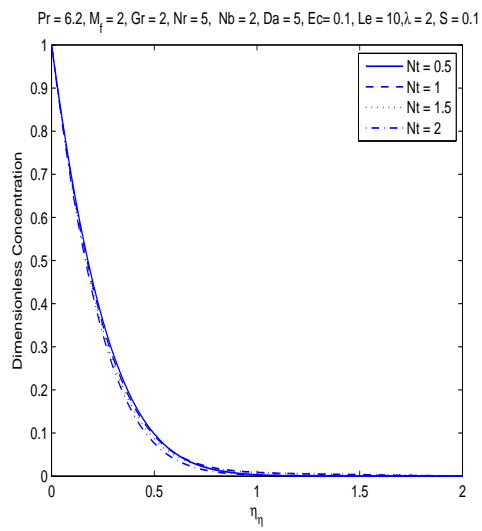Figure 4.5: Computational velocity and temperature profiles against variation values of Gr.

Pr = 6.2, M$_f$ = 2, Gr = 2, Nr = 5, Nb = 2, Da = 5, Ec= 0.1, Le = 10,λ = 2, S = 0.1

Pr = 6.2, M$_f$ = 2, Gr = 5, Nr = 5, Da = 5, Nt = 2, Ec= 0.1, Le = 2,λ = 3, S = 0.1

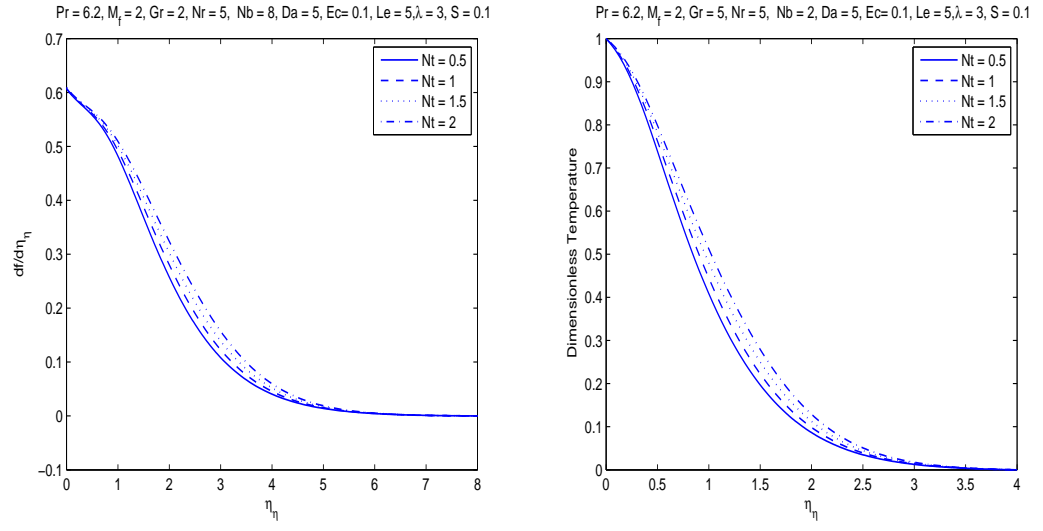Figure 4.6: Computational concentration profiles against variation values of Nt and Nb.

Figure 4.7: Computational velocity and temperature profiles against variation values of Nt.
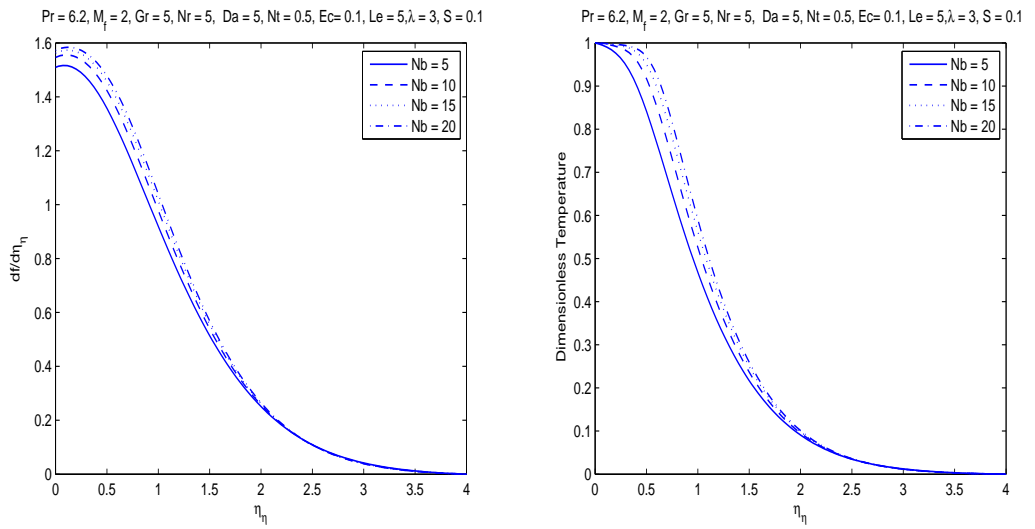
Figure 4.8: Computational velocity and temperature profiles against variation values of Nb.
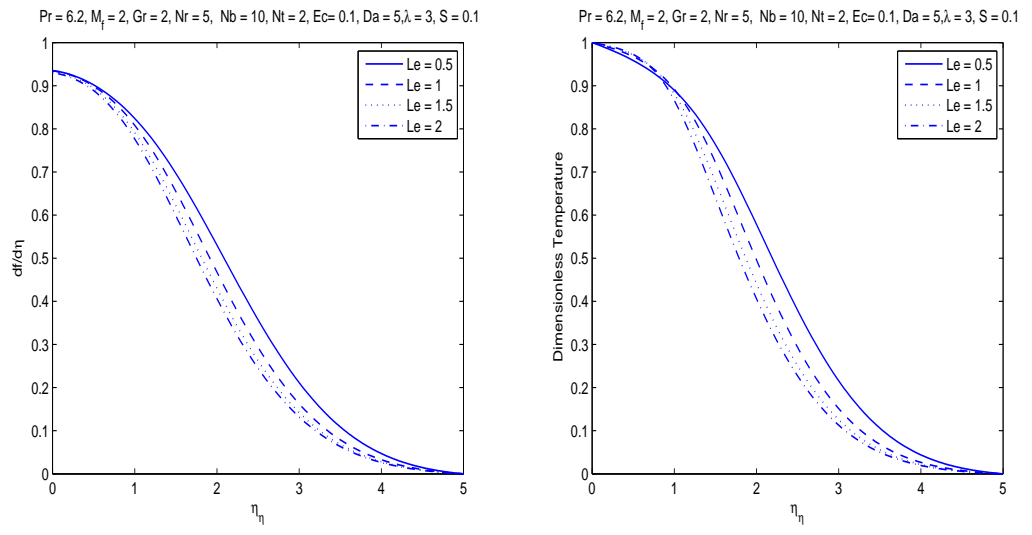
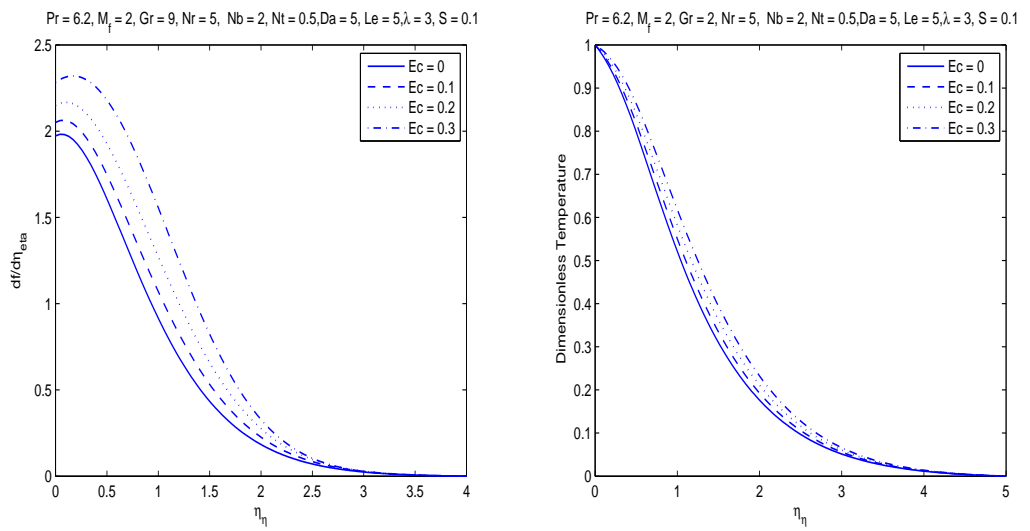Figure 4.9: Computational velocity and temperature profiles against variation values of *Le*.

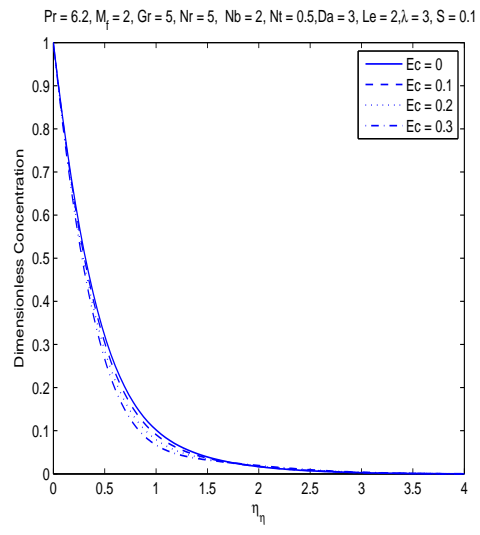Figure 4.10: Computational velocity and temperature profiles against variation values of *Ec*.

Figure 4.11: Computational velocity and temperature profiles against variation values of Ec.

Chapter 5

Conclusions

In this chapter, we conclude all the results of previous chapters. In this study, a mathematical model for nanofluid flow considering MHD, radiation, porosity has been discussed. In first extension, there is huge impact on concentration profile with and with out Grashof number. It is depicted that concentration boundary layer thickness is higher in the absence of Grashof number as compare to that of other values. The influence of unsteady parameter on temperature and thermal boundary layer thickness is also significant. By increasing τ the temperature profile increase. Also large value of Nt dampen the temperature profile with an incremental τ. The skin friction coefficient increases while there is reduction in both local Nusselt number and local Sherwood number with an incremental magnetic parameter. In second extension, there is significant increase of Sherwood number by Lewis number. It is depicted that without Eckert number the behavior of velocity at the surface is low then increase significantly with Eckert number. Also the thermal boundary layer thickness increase due to an increase of magnetic parameter. We successfully developed and applied the simplified FDM for the current problem. To validate we compare simplified FDM results with *bvp4c* as well as with literature which gives a good account agreement with each other.

Bibliography

[1] Crane, L. J. (1970). Flow past a stretching plate. Zeitschrift fÃijr angewandte Mathematik und Physik ZAMP, 21(4), 645-647.

[2] Makinde, O. D., and Aziz, A. (2011). Boundary layer flow of a nanofluid past a stretching sheet with a convective boundary condition. International Journal of Thermal Sciences, 50(7), 1326-1332.

[3] Mustafa, M., Hayat, T., and Obaidat, S. (2013). Boundary layer flow of a nanofluid over an exponentially stretching sheet with convective boundary conditions. International Journal of Numerical Methods for Heat and Fluid Flow, 23(6), 945-959.

[4] Gupta, P. S., and Gupta, A. S. (1977). Heat and mass transfer on a stretching sheet with suction or blowing. The Canadian Journal of Chemical Engineering, 55(6), 744-746.

[5] Choi, S. U., and Eastman, J. A. (1995). Enhancing thermal conductivity of fluids with nanoparticles (No. ANL/MSD/CP-84938; CONF-951135-29). Argonne National Lab., IL (United States).

[6] Sheikholeslami, M., and Bhatti, M. M. (2017). Forced convection of nanofluid in presence of constant magnetic field considering shape effects of nanoparticles. International Journal of Heat and Mass Transfer, 111, 1039-1049.

[7] Sheikholeslami, M. (2018). CuO-water nanofluid flow due to magnetic field inside a porous media considering Brownian motion. Journal of Molecular Liquids, 249, 921-929.

[8] Xenos, M., Kafoussias, N., and Karahalios, G. (2001). Magnetohydrodynamic compressible laminar boundary-layer adiabatic flow with adverse pressure gradient and continuous or localized mass transfer. Canadian Journal of Physics, 79(10), 1247-1263.

[9] Reddy, J. R., Kumar, K. A., Sugunamma, V., and Sandeep, N. (2018). Effect of cross diffusion on MHD non-Newtonian fluids flow past a stretching sheet with non-uniform heat source/sink: A comparative study. Alexandria engineering journal, 57(3), 1829-1838.

[10] Mishra, U., and Singh, G. (2014). Dual solutions of mixed convection flow with momentum and thermal slip flow over a permeable shrinking cylinder. Computers and Fluids, 93, 107-115.

[11] Hadjiconstantinou, N. G. (2003). Comment on CercignaniâĂŹs second-order slip coefficient. Physics of Fluids, 15(8), 2352-2354.

[12] Hadjiconstantinou, N. G. (2006). The limits of Navier-Stokes theory and kinetic extensions for describing small-scale gaseous hydrodynamics. Physics of Fluids, 18(11), 111301.

[13] Fang, T., Yao, S., Zhang, J., and Aziz, A. (2010). Viscous flow over a shrinking sheet with a second order slip flow model. Communications in Nonlinear Science and Numerical Simulation, 15(7), 1831-1842.

[14] Ullah, A., Alzahrani, E., Shah, Z., Ayaz, M., and Islam, S. (2019). Nanofluids Thin Film Flow of Reiner-Philippoff Fluid over an Unstable Stretching Surface with Brownian Motion and Thermophoresis Effects. Coatings, 9(1), 21.

[15] Khan, M. S., Karim, I., Ali, L. E., and Islam, A. (2012). Unsteady MHD free convection boundary-layer flow of a nanofluid along a stretching sheet with thermal radiation and viscous dissipation effects. International Nano Letters, 2(1), 24.

[16] Ibrahim, W., and Shankar, B. (2013). MHD boundary layer flow and heat transfer of a nanofluid past a permeable stretching sheet with velocity, thermal and solutal slip boundary conditions. Computers and Fluids, 75, 1-10.

[17] Makinde, O. D., Khan, W. A., and Khan, Z. H. (2013). Buoyancy effects on MHD stagnation point flow and heat transfer of a nanofluid past a convectively heated stretching/shrinking sheet. International Journal of Heat and Mass Transfer, 62, 526-533.

[18] Ali, M., and Al-Yousef, F. (1998). Laminar mixed convection from a continuously moving vertical surface with suction or injection. Heat and Mass Transfer, 33(4), 301-306.

[19] Partha, M. K., Murthy, P. V. S. N., and Rajasekhar, G. P. (2005). Effect of viscous dissipation on the mixed convection heat transfer from an exponentially stretching surface. Heat and Mass Transfer, 41(4), 360-366.

[20] Gebhart, B. (1962). Effects of viscous dissipation in natural convection. Journal of fluid Mechanics, 14(2), 225-232.

[21] Gebhart, B., and Mollendorf, J. (1969). Viscous dissipation in external natural convection flows. Journal of fluid Mechanics, 38(1), 97-107.

[22] Magyari, E., and Keller, B. (1999). Heat and mass transfer in the boundary layers on an exponentially stretching continuous surface. Journal of Physics D: Applied Physics, 32(5), 577.

[23] Seth, G. S., Bhattacharyya, A., Kumar, R., and Chamkha, A. J. (2018). Entropy generation in hydromagnetic nanofluid flow over a non-linear stretching sheet with NavierâĂŹs velocity slip and convective heat transfer. Physics of Fluids, 30(12), 122003.

[24] Makinde, O. D., Khan, Z. H., Ahmad, R., and Khan, W. A. (2018). Numerical study of unsteady hydromagnetic radiating fluid flow past a slippery stretching sheet embedded in a porous medium. Physics of Fluids, 30(8), 083601.

[25] Hamid, A., and Khan, M. (2018). Unsteady mixed convective flow of Williamson nanofluid with heat transfer in the presence of variable thermal conductivity and magnetic field. Journal of Molecular Liquids, 260, 436-446.

[26] Jafaryar, M., Sheikholeslami, M., and Li, Z. (2018). CuO-water nanofluid flow and heat transfer in a heat exchanger tube with twisted tape turbulator. Powder technology, 336, 131-143.

[27] Hamid, A., and Khan, M. (2018). Impacts of binary chemical reaction with activation energy on unsteady flow of magneto-Williamson nanofluid. Journal of Molecular Liquids, 262, 435-442.

[28] Khan, M., and Hafeez, A. (2017). A review on slip-flow and heat transfer performance of nanofluids from a permeable shrinking surface with thermal radiation: dual solutions. Chemical Engineering Science, 173, 1-11.

[29] Qing, J., Bhatti, M., Abbas, M., Rashidi, M., and Ali, M. (2016). Entropy generation on MHD Casson nanofluid flow over a porous stretching/shrinking surface. Entropy, 18(4), 123.

[30] Hosseini, S. R., Sheikholeslami, M., Ghasemian, M., and Ganji, D. D. (2018). Nanofluid heat transfer analysis in a microchannel heat sink (MCHS) under the effect of magnetic field by means of KKL model. Powder Technology, 324, 36-47.

[31] Eid, M. R. (2016). Chemical reaction effect on MHD boundary-layer flow of two-phase nanofluid model over an exponentially stretching sheet with a heat generation. Journal of Molecular Liquids, 220, 718-725.

[32] Afify, A. A., and Elgazery, N. S. (2016). Effect of a chemical reaction on magneto-hydrodynamic boundary layer flow of a Maxwell fluid over a stretching sheet with nanoparticles. Particuology, 29, 154-161.

[33] Prasad, K. V., Vajravelu, K.,and Datti, P. S. (2010). Mixed convection heat transfer over a non-linear stretching surface with variable fluid properties. International Journal of non-linear Mechanics, 45(3), 320-330.

[34] Afzal, N. (2010). Momentum and thermal boundary layers over a two-dimensional or axisymmetric non-linear stretching surface in a stationary fluid. International Journal of Heat and Mass Transfer, 53(1-3), 540-547.

[35] Nandeppanavar, M. M., Vajravelu, K., Abel, M. S., and Ng, C. O. (2011). Heat transfer over a nonlinearly stretching sheet with non-uniform heat source and variable wall temperature. International Journal of Heat and Mass Transfer, 54(23-24), 4960-4965.

[36] Nadeem, S., and Lee, C. (2012). Boundary layer flow of nanofluid over an exponentially stretching surface. Nanoscale research letters, 7(1), 94.

[37] Mohamad, R. B., Kandasamy, R., and Muhaimin, I. (2013). Enhance of heat transfer on unsteady Hiemenz flow of nanofluid over a porous wedge with heat source/sink due to solar energy radiation with variable stream condition. Heat and Mass Transfer, 49(9), 1261-1269.

[38] Makinde, O. D., Khan, W. A., and Culham, J. R. (2016). MHD variable viscosity reacting flow over a convectively heated plate in a porous medium with thermophoresis and radiative heat transfer. International Journal of Heat and Mass Transfer, 93, 595-604.

[39] S. Rosseland, Astrophysik aud Atom-Theoretische Grundlagen (Springer, Berlin, 1931), pp. 41âĂŞ44.

[40] Tyagi, H. (2008). Radiative and combustion properties of nanoparticle-laden liquids. Arizona State University.

[41] Eegunjobi, A. S., Makinde, O. D., and Jangili, S. (2017). Unsteady MHD chemically reacting and radiating mixed convection slip flow past a stretching surface in a porous medium. In Defect and Diffusion Forum (Vol. 377, pp. 200-210). Trans Tech Publications.

[42] Makinde, O. D., Mabood, F., Khan, W. A., and Tshehla, M. S. (2016). MHD flow of a variable viscosity nanofluid over a radially stretching convective surface with radiative heat. Journal of Molecular Liquids, 219, 624-630.

[43] Khan, W. A., Makinde, O. D., and Khan, Z. H. (2016). Non-aligned MHD stagnation point flow of variable viscosity nanofluids past a stretching sheet with radiative heat. International Journal of Heat and Mass Transfer, 96, 525-534.

[44] LeVeque, R. J. (2007). Finite difference methods for ordinary and partial differential equations: steady-state and time-dependent problems (Vol. 98). Siam.

[45] Buongiorno, J. (2006). Convective transport in nanofluids. Journal of heat transfer, 128(3), 240-250.

[46] Na, T. Y. (Ed.). (1980). Computational methods in engineering boundary value problems (Vol. 145). Academic Press.

[47] Shampine, L. F., Kierzenka, J., and Reichelt, M. W. (2000). Solving boundary value problems for ordinary differential equations in MATLAB with bvp4c. Tutorial notes, 2000, 1-27.

[48] Sharif, Razia and Farooq, M Asif and Mushtaq, Asif (2019). Magnetohydrodynamic Study of Variable Fluid Properties and Their Impact on Nanofluid Over an Exponentially Stretching Sheet . Journal of Nanofluids, 8(6), 1249–1259.

[49] Gschwendtner, M. A. (2004). The Eckert number phenomenon: Experimental investigations on the heat transfer from a moving wall in the case of a rotating cylinder. Heat and mass transfer, 40(6-7), 551-559.